



**NAVAL
POSTGRADUATE
SCHOOL**

MONTEREY, CALIFORNIA

THESIS

**MODEL TO CALCULATE THE EFFECTIVENESS
OF AN AIRBORNE JAMMER ON ANALOG
COMMUNICATIONS**

by

Narciso A. Vingson, Jr.

Vaqar Muhammad

September 2005

Thesis Advisor:

Jovan E. Lebaric

Second Reader:

Richard W. Adler

Approved for public release; distribution is unlimited

THIS PAGE INTENTIONALLY LEFT BLANK

REPORT DOCUMENTATION PAGE			Form Approved OMB No. 0704-0188	
Public reporting burden for this collection of information is estimated to average 1 hour per response, including the time for reviewing instruction, searching existing data sources, gathering and maintaining the data needed, and completing and reviewing the collection of information. Send comments regarding this burden estimate or any other aspect of this collection of information, including suggestions for reducing this burden, to Washington headquarters Services, Directorate for Information Operations and Reports, 1215 Jefferson Davis Highway, Suite 1204, Arlington, VA 22202-4302, and to the Office of Management and Budget, Paperwork Reduction Project (0704-0188) Washington DC 20503.				
1. AGENCY USE ONLY (Leave blank)		2. REPORT DATE September 2005	3. REPORT TYPE AND DATES COVERED Master's Thesis	
4. TITLE AND SUBTITLE: Model to Calculate the Effectiveness of an Airborne Jammer on Analog Communications			5. FUNDING NUMBERS	
6. AUTHOR(S) Narciso A. Vingson, Jr. and Vaqar Muhammad				
7. PERFORMING ORGANIZATION NAME(S) AND ADDRESS(ES) Naval Postgraduate School Monterey, CA 93943-5000			8. PERFORMING ORGANIZATION REPORT NUMBER	
9. SPONSORING /MONITORING AGENCY NAME(S) AND ADDRESS(ES) N/A			10. SPONSORING/MONITORING AGENCY REPORT NUMBER	
11. SUPPLEMENTARY NOTES The views expressed in this thesis are those of the author and do not reflect the official policy or position of the Department of Defense or the U.S. Government.				
12a. DISTRIBUTION / AVAILABILITY STATEMENT Approved for public release; distribution is unlimited			12b. DISTRIBUTION CODE	
13. ABSTRACT (maximum 200 words) The objective of this study is to develop a statistical model to calculate the effectiveness of an airborne jammer on analog communication and broadcast receivers, such as AM and FM Broadcast Radio and Television receivers. During the development the required power margin in dB, or equivalently, the required linear ratio, between the jammer power and the carrier power at the target receiver input was first determined. Subsequently, using probabilities that the jammer power will exceed the target signal's carrier power, the required power margin was calculated. This power margin was determined by statistical techniques to predict the propagation characteristics of communication and broadcast signals, such as Log-Normal Shadowing, and Small-Scale Fading. From the model, it was determined that it is difficult to achieve high probabilities of exceeding the required jamming margins with a single jammer. Hence, the use of spatial diversity jamming is recommended, that is, using two or more jammers spaced sufficiently far apart from each other, such that their jamming signals at the targeted area are de-correlated due to the differences in their respective angles of arrival.				
14. SUBJECT TERMS Airborne Jammer, Analog Communications, Broadcast Receivers, Propagation Model, Large- Scale Path Loss, Log-Normal Shadowing, Small-Scale Fading			15. NUMBER OF PAGES 77	
			16. PRICE CODE	
17. SECURITY CLASSIFICATION OF REPORT Unclassified	18. SECURITY CLASSIFICATION OF THIS PAGE Unclassified	19. SECURITY CLASSIFICATION OF ABSTRACT Unclassified	20. LIMITATION OF ABSTRACT UL	

THIS PAGE INTENTIONALLY LEFT BLANK

Approved for public release; distribution is unlimited

**MODEL TO CALCULATE THE EFFECTIVENESS OF AN AIRBORNE
JAMMER ON ANALOG COMMUNICATIONS**

Narciso A. Vingson, Jr.
Commander, Philippine Navy
B.S., Philippine Military Academy, 1985

Vaqar Muhammad
Lieutenant Commander, Pakistan Navy
B.S., Karachi University, 1994

Submitted in partial fulfillment of the
requirements for the degree of

MASTER OF SCIENCE IN SYSTEMS ENGINEERING

from the

**NAVAL POSTGRADUATE SCHOOL
September 2005**

Authors: Narciso A Vingson, Jr.
Vaqar Muhammad

Approved by: Jovan E. Lebaric
Thesis Advisor

Richard W. Adler
Second Reader/Co-Advisor

Dan C. Boger
Chairman, Department of Information Sciences

THIS PAGE INTENTIONALLY LEFT BLANK

ABSTRACT

The objective of this study is to develop a statistical model to calculate the effectiveness of an airborne jammer on analog communication and broadcast receivers, such as AM and FM Broadcast Radio and Television receivers.

During the development the required power margin in dB, or equivalently, the required linear ratio, between the jammer power and the carrier power at the target receiver input was first determined. Subsequently, using probabilities that the jammer power will exceed the target signal's carrier power, the required power margin was calculated.

This power margin was determined by statistical techniques to predict the propagation characteristics of communication and broadcast signals, such as Log-Normal Shadowing, and Small-Scale Fading.

From the model, it was determined that it is difficult to achieve high probabilities of exceeding the required jamming margins with a single jammer. Hence, the use of spatial diversity jamming is recommended, that is, using two or more jammers spaced sufficiently far apart from each other, such that their jamming signals at the targeted area are de-correlated due to the differences in their respective angles of arrival.

THIS PAGE INTENTIONALLY LEFT BLANK

TABLE OF CONTENTS

I.	INTRODUCTION.....	1
A.	BACKGROUND	1
B.	OBJECTIVE	1
C.	JAMMING STRATEGY.....	2
II.	RADIO PROPAGATION	5
A.	THE COMMUNICATIONS CHANNEL.....	5
1.	The Propagation Channel	6
2.	The Radio Channel	6
3.	The Modulation Channel	6
B.	PATH LOSS	7
C.	PROPAGATION PREDICTION MODELS.....	8
1.	Free-space Propagation Model	8
2.	Two-Ray Propagation Model.....	10
3.	Okumura-Hata Empirical Formula.....	12
III.	RECEIVER INPUT SIGNAL-TO-NOISE RATIO (SNR_{IN})	17
A.	RECEIVED INPUT SIGNAL POWER.....	17
B.	RECEIVER INPUT NOISE POWER	18
C.	INPUT SIGNAL-TO-NOISE RATIO.....	20
IV.	RECEIVER OUTPUT SIGNAL-TO-NOISE RATIO (SNR_{OUT})	25
A.	AMPLITUDE MODULATION – COHERENT DETECTION.....	25
B.	AMPLITUDE MODULATION – NON-COHERENT DETECTION.....	28
1.	Double-Sideband Large Carrier (DSB-LC or AM).....	29
2.	Vestigial Sideband Large Carrier (VSB-LC).....	34
C.	FREQUENCY MODULATION.....	36
V.	JAMMING OBJECTIVES FOR TARGETED SIGNALS.....	43
A.	AMPLITUDE MODULATED (AM) BROADCAST RADIO AND BROADCAST TV	44
B.	FREQUENCY MODULATED (FM) BROADCAST RADIO	44
C.	BROADCAST TV (VIDEO)	44
D.	BROADCAST TV (AUDIO).....	45
VI.	DEVELOPMENT OF THE MODEL	47
A.	SITE-SPECIFIC AND STATISTICAL PREDICTIONS	47
B.	LOG-NORMAL SHADOWING	48
C.	SMALL SCALE FADING	50
D.	THE PROPOSED STATISTICAL MODEL	52
VII.	CONCLUSIONS	57
A.	CONCLUSIONS	57
B.	RECOMMENDATIONS.....	57
	LIST OF REFERENCES.....	59
	INITIAL DISTRIBUTION LIST	61

THIS PAGE INTENTIONALLY LEFT BLANK

LIST OF FIGURES

Figure 1.	Communication Channel	2
Figure 2.	Input and Output SNR	3
Figure 3.	Jamming Scenario Geometry	3
Figure 4.	The Communications Channel (After Ref. [3].)	6
Figure 5.	Path Loss Model (After Ref. [4].)	8
Figure 6.	Free Space Propagation Path	10
Figure 7.	Two-Ray Model (After Ref. [5].)	11
Figure 8.	Two-Ray Propagation Path Loss	12
Figure 9.	Okumura-Hata Propagation Path Loss.....	14
Figure 10.	Fresnel Zone (FZ) (After Ref. [4].).....	15
Figure 11.	SNR at the Input for Free Space Model with Varying Power	21
Figure 12.	SNR at the Input for Free Space Model with Varying Transmitted Frequency.....	22
Figure 13.	SNR at the Input for Free Space Model with Varying Gain.....	22
Figure 14.	SNR at the Input for Two Ray Model with Varying Power	23
Figure 15.	SNR at the Input for Two Ray Model with Varying Gain.....	23
Figure 16.	SNR at the Input for Two Ray Model with Varying Antenna Heights	24
Figure 17.	Block Diagram for Coherent Demodulation.....	26
Figure 18.	Block Diagram for Envelope AM Detection	30
Figure 19.	Envelope Detection Plot (From Ref. [11].).....	32
Figure 20.	Square Law Detection Plot (From Ref. [11].).....	33
Figure 21.	Illustrative FM Waveform	36
Figure 22.	Quieting Threshold (After Ref. [13].).....	39
Figure 23.	Preemphasis and Deemphasis Networks in FM Transmission (After Ref. [15].).....	39
Figure 24.	Effect of Broadband Masking Noise (From Ref. [12].).....	43
Figure 25.	Image Quality versus SNR (After Ref. [18].).....	45
Figure 26.	Spatial Diversity Jamming.....	58

THIS PAGE INTENTIONALLY LEFT BLANK

LIST OF TABLES

Table 1.	Threshold	46
Table 2.	Jamming Margin	46

THIS PAGE INTENTIONALLY LEFT BLANK

ACKNOWLEDGMENTS

The authors would like to thank their families for their invaluable morale support during the formulation of this thesis.

Likewise, we are also grateful to the following:

- Professor Jovan E. Lebaric, Thesis Advisor, who magnanimously providing all the technical inputs and expert opinion into the design and formulation of the project;
- Professor Richard W. Adler, Co-Advisor, for painstakingly reviewing all the contents of the thesis to be in suitable form and substance;
- Professor Dan C. Boger, Chairman, Department of Information Sciences, for maintaining an internationally respected research program in selected areas of information sciences, systems, and operations.
- Professor David Jenn, Academic Associate, for his continuous guidance in pursuing our career path under the EW 596 Curriculum.

Our special thanks also go to Nita Maniego and Ann Wells for carefully editing and formatting our work according to the desired format.

THIS PAGE INTENTIONALLY LEFT BLANK

I. INTRODUCTION

A. BACKGROUND

Analog radio is a broadcast technology where anyone within reception range has access to the transmitted signal with little effort. Communicating privately with another person using two-way radio is the same for commercial radio transmission, only at a different frequency. It is inherently a communication medium which is vulnerable to interruption.

Generally, jamming prevents an adversary from using their radar or radio for either offensive or defensive purposes, by placing an interfering signal into the enemy receiver along with the desired signal. Jammers usually use a high power transmitter that mimics the frequencies and modulation used by an opponent to disrupt their receivers and to corrupt the expected information. Jamming can also be used to add spurious signals to radar system returns, fooling the receiving radar to think there are more, or fewer, targets in an area. In some cases, particularly in depriving a user of radio communication, complete transmissions are recorded, altered and retransmitted, making the recipient unsure of the quality of the data. [1]

B. OBJECTIVE

The objective of this study is to develop a statistical model to calculate the effectiveness of an airborne jammer on communications and broadcast receivers.

This model should:

- determine the required power margin, M , in dB (or equivalently, the required linear ratio) between the jammer power and the carrier power at the target receiver input and to
- calculate the probability that the jammer power will exceed the target signal's carrier power by the required margin, M .

The following are the target signals:

- Amplitude Modulated (AM) Broadcast Radio,
- Frequency Modulated (FM) Broadcast Radio,
- Frequency Modulated (FM) Communications Radio, and

- Broadcast TV.

C. JAMMING STRATEGY

The pre-detection measure of signal quality is the carrier-to noise-ratio power ratio (CNR). The post-detection measure of signal quality is the signal-to-noise power ratio (SNR). The jamming objective is to degrade the CNR and SNR. The pre-detection measure of jammer effectiveness is the carrier-to-jam-plus-noise power ratio, CJR. The composite carrier-to-jam-plus-noise power ratio, CNJR, is given by

$$\frac{1}{CNJR} = \frac{1}{CJR} + \frac{1}{CNR} .$$

This jamming strategy is based on a communication channel as illustrated in Figure 1. The objective is to determine the signal (recovered message) to noise ratio at the receiver output, for a known signal-to-noise ratio at the receiver input.

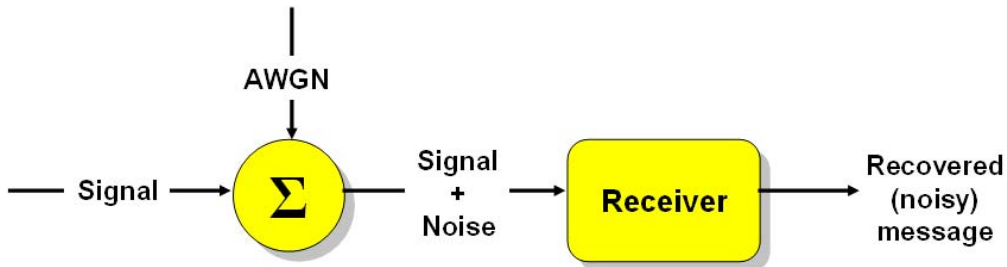


Figure 1. Communication Channel

The modulated signal is assumed to be corrupted by additive, white Gaussian noise (AWGN). The receiver is assumed to be noise-free. The effect of the receiver noise is accounted for by adjusting the input noise power density accordingly. The receiver bandwidth is known.

The input SNR is defined as the ratio of the received (modulated) signal power to the noise power within the receiver bandwidth. The received signal power can be calculated from the known transmitter power, transmitter antenna gain, receiver antenna gain, and the path loss between the transmitter and the receiver. The input noise power can be calculated from the known system temperature and the receiver bandwidth.

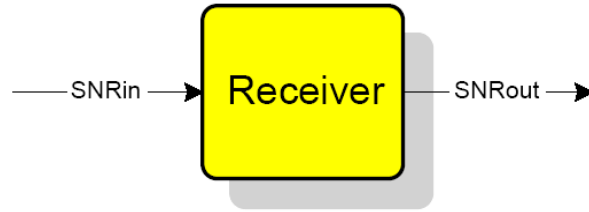


Figure 2. Input and Output SNR

In order for the jammer to be effective, its signal must enter the enemy's receiver through the associated antenna, input filters, and processing gates. This, in turn, depends on the jammer power density transmitted in the direction of the receiver and the distance and the propagation conditions between the jammer and the receiver. The Jamming Scenario Geometry, shown in Figure 3, illustrates this approach.

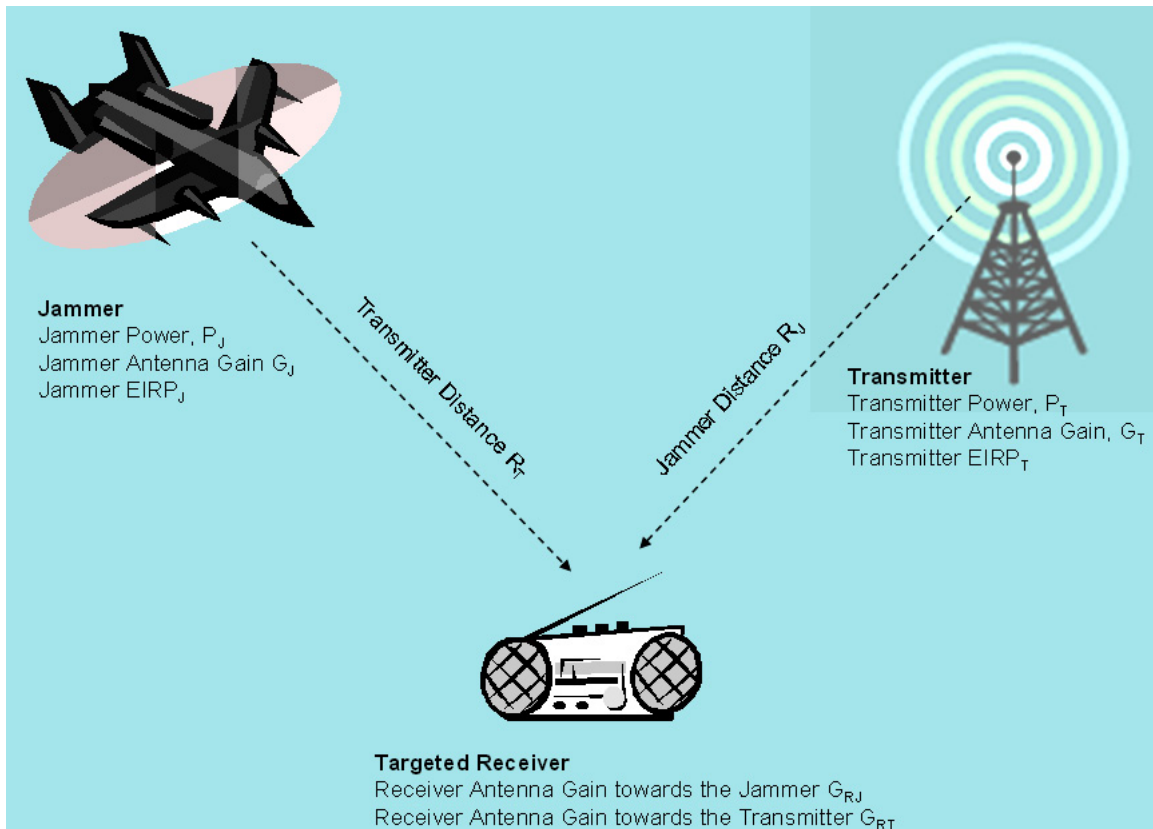


Figure 3. Jamming Scenario Geometry

The following chapters explain in detail how the objective of this study is met. It contains the development of a statistical model for calculating the effectiveness of an airborne jammer on communications and broadcast receivers.

II. RADIO PROPAGATION

This chapter introduces the basic parameters that characterize propagation phenomena in the radio environment. It begins by reviewing the elements of the communications channel, radio wave degradation that affects the signal quality as the wave propagates through space, and the application of the Friis free-space transmission formula which constitutes the basis for the propagation path loss models presented in this chapter.

The Radio propagation models can be divided into two groups, namely, theoretical models and empirical models. The theoretical models are usually described by means of closed-form expressions, whereas the empirical ones are based on fitting curve-fitting or analytical expressions that recreate a set of data derived from field measurements, taken at different conditions. In the first case, many approximations are carried out, so that the models may not be directly applicable to real situations. In the second case, many parameters are taken into account, and the models very complex. A combination of these groups of models gives rise to a simplified prediction model with acceptable results, if high accuracy is not required. The various parameters affecting the radio propagation are also discussed and analyzed [2].

A. THE COMMUNICATIONS CHANNEL

The communications channel is the link between two points along a communications path. For radio-frequencies (RF) the primary propagation medium is the atmosphere, and wave attenuation is due to geometric spreading, multipath wave interference, and absorptive loss in the medium. Figure 4 illustrates the composition of the RF channel [3]:

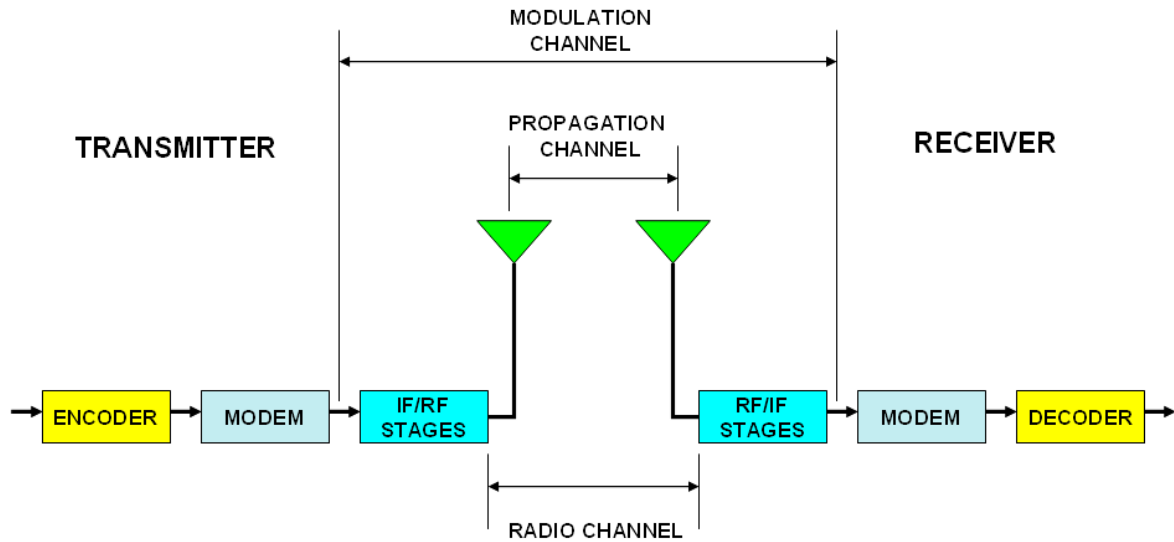


Figure 4. The Communications Channel (After Ref. [3].)

1. The Propagation Channel

The propagation channel is the physical medium that supports the electromagnetic wave propagation between a transmit and a receive antenna, which is everything that influences propagation between two antennas.

2. The Radio Channel

The transmitter antenna, propagation channel and receiver antenna viewed collectively, constitute the radio channel. The propagation channel is reciprocal, thus the reciprocity of the radio channel depends on the antennas used. It can be shown that the antennas exhibit the same transmit and receive radiation patterns in free space if they are bilateral, liner and passive. Under these circumstances the antennas are reciprocal, and therefore, so is the radio channel.

3. The Modulation Channel

The modulation channel extends from output of the modulator to the input of the demodulator and is composed of the transmitter front-end, receiver front-end, and the radio channel. It represents the complete signal path between the output of the modulator and the input to the demodulator [3].

B. PATH LOSS

During propagation between transmitting and receiving antennas, the radio signal experiences attenuation due to a number of phenomena, such as free-space loss, refraction, reflection, aperture-medium coupling loss, and absorption. This degradation affects the signal quality and can induce errors in received messages that leads to a loss of information. The signal degradation resulting from propagation in the radio channel can be classified by type such as multipath, shadowing and 'large scale effects'.

1. Multipath is a phenomenon where the transmitted signal arrives at the receiver from various directions over a multiplicity of paths due to some obstacles and reflections in the propagation channel. These reflected waves can add to or subtract from with the direct wave, which causes significant changes in the received signal.

2. Shadowing is a 'medium-scale' effect, which describes the variation of the signal power at a constant distance from the transmitter, but in different directions. This is caused by variations in building height, size and material, separation between buildings, presence of trees, etc. In response to the variations in the nearby obstructions, there will be a change in the average value which the rapid fluctuations take place.

3. The 'large-scale' effects of path losses cause the received power to vary gradually due to signal attenuation determined by the geometry of the path profile in its entirety. It is concerned with predicting the mean signal strength as a function of transmitter-receiver (T-R) separation distance (d) over T-R separations of hundreds, thousands, or millions of wavelengths. The most appropriate path loss model depends on the location of the receiving antenna as illustrated in Figure 5 [4]:

- a. Location 1: Free space loss is likely to give an accurate estimate of path loss.
- b. Location 2: A strong line-of-sight component is present, but ground reflections can significantly influence path loss.
- c. Location 3: Plane earth loss must be corrected for significant diffraction losses, such as that caused by trees blocking the direct line of sight.

- d. Location 4: A simple diffraction model is likely to give an accurate estimate of path loss.
- e. Location 5: Loss prediction is fairly difficult and unreliable since multiple diffractions are involved.

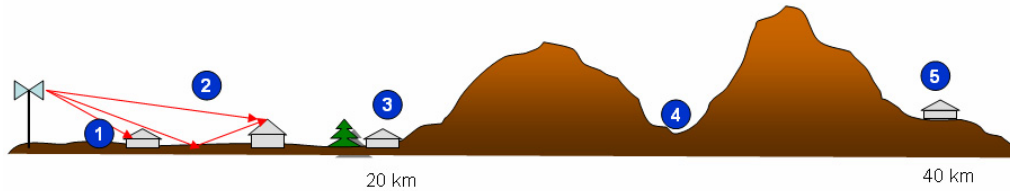


Figure 5. Path Loss Model (After Ref. [4].)

C. PROPAGATION PREDICTION MODELS

The three commonly used propagation models for large-scale path loss prediction are: Free-space propagation, Two-Ray propagation, and the Okumura-Hata empirical formula.

1. Free-space Propagation Model

The primary propagation medium in radiowave propagation is the atmosphere, and wave attenuation is due to geometric spreading and absorptive loss in the medium.

The basic free-space propagation attenuation is due to the geometric spherical expansion of the waves, so attenuation is inversely proportional to the distance squared and is referred to as the *Friis Free Space Equation* [5]

$$P_r = \frac{P_t G_t G_r}{\left(\frac{4\pi x d}{\lambda}\right)^2}, \quad (2.1)$$

or in decibels

$$P_{r_{dBW}} = P_{t_{dBm}} + G_{t_{dBi}} + G_{r_{dBi}} + 20 \log_{10} \left(\frac{\lambda}{4\pi}\right) - 20 \log_{10}(d), \quad (2.2)$$

where

- P_r is received power in dBm,

- P_t is transmitted power in dBm,
- G_t is transmit antenna gain (isotropic),
- G_r is receive antenna gain (isotropic),
- λ is wavelength (m), and
- d is Tx-Rx separation in same units as wavelength.

Free Space Path Loss

The Free space transmission formula gives an inverse square relationship between the received power and the T-R separation distance. This implies the received power decays at a rate of 20 dB/decade with the distance.

The path loss is defined as the difference between the effective transmitted power and the received power and may include the effect of the antenna gains. It is given in decibels as

$$L_{fs} = -10 \log_{10} \left(\frac{P_r}{P_t} \right) = -10 \log_{10} \left(\frac{G_t G_r \lambda^2}{(4\pi)^2 d^2} \right), \quad (2.3)$$

or for direct line of sight paths and no atmospheric absorption [6]

$$L_{fs} = 20 \log_{10} \left(\frac{4\pi d}{\lambda} \right) = 20 \log_{10} \left(\frac{4\pi 1000d}{228.8f} \right) \quad (2.4)$$

$$= 32.45 + 20 \log_{10}(d) + 20 \log_{10}(f),$$

where d is the T-R separation distance in km and f is the frequency in MHz.

Shown in Figure 6 is the propagation path loss using Free Space model at different frequencies as a function of distance.

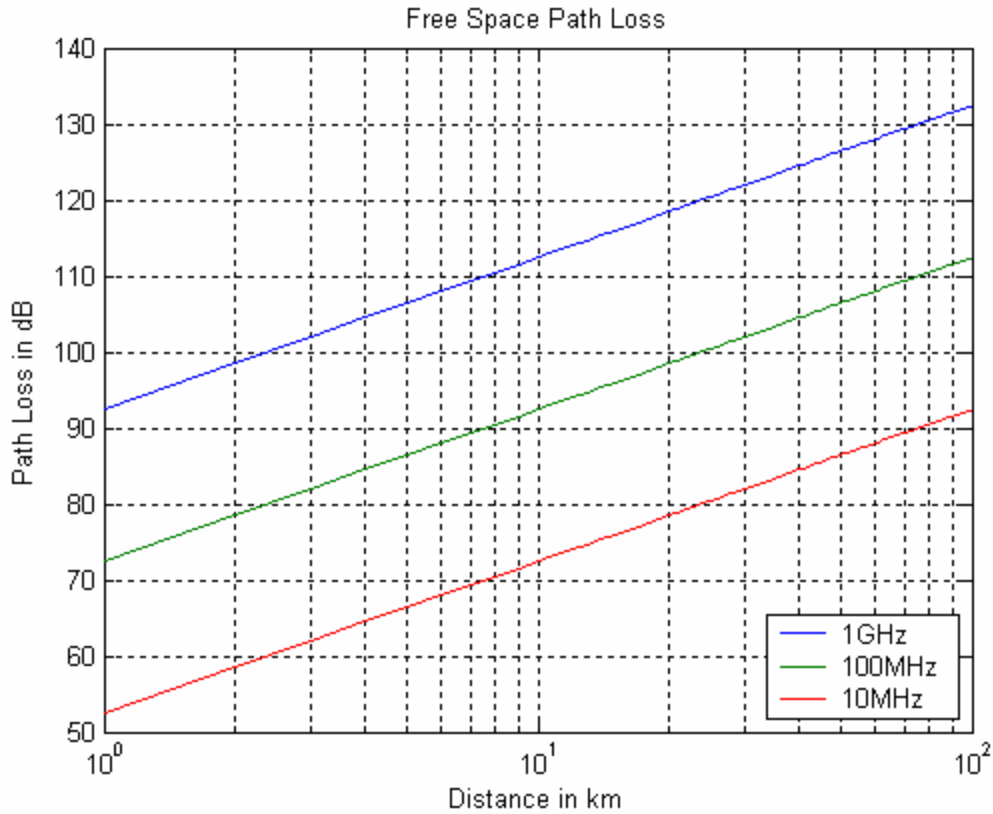


Figure 6. Free Space Propagation Path

2. Two-Ray Propagation Model

Radio propagation between two points that are near the ground involves an expanding spherical wave propagating from the source antenna to the target antenna. Because of the air-ground boundary, ground currents are induced that then reradiated and combine as complex vectors with the source spherical wave. In this case, the two-ray model is commonly used. As shown in Figure 7, the two-ray model generally applies at lower frequencies and altitudes.

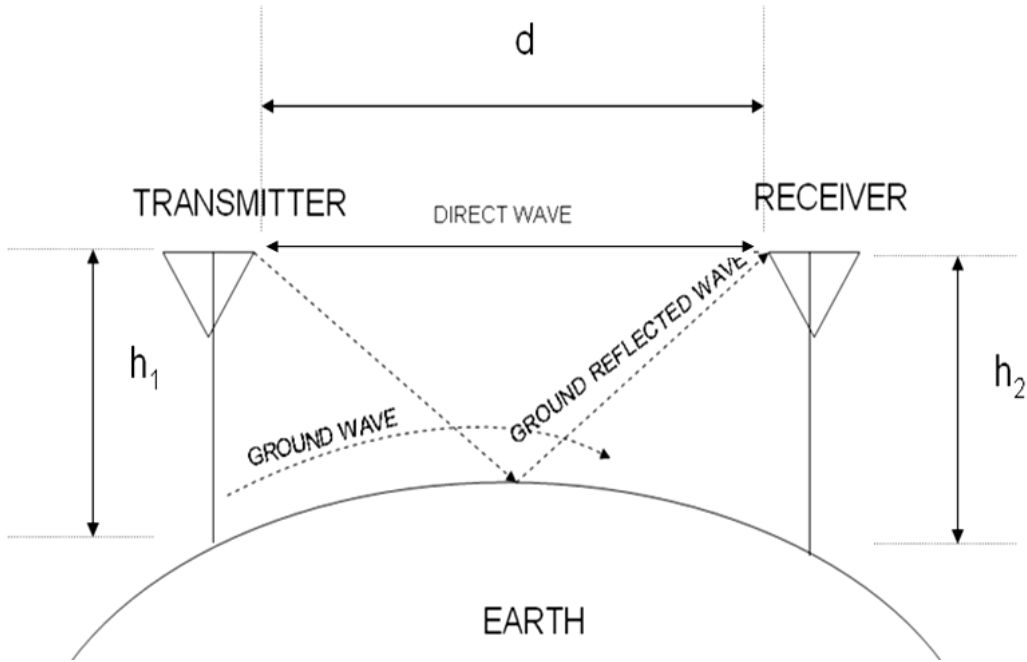


Figure 7. Two-Ray Model (After Ref. [5].)

The propagation loss for two-ray propagation is independent of frequency which can be approximated as [6]

$$L_{two-ray} \approx \left(\frac{d^2}{h_1 h_2} \right) = \frac{d^4}{h_1^2 h_2^2}, \quad (2.5)$$

or in decibel form,

$$L_{two-ray} \approx 120 + 40 \log_{10}(d) - 20 \log_{10}(h_1) - 20 \log_{10}(h_2), \quad (2.6)$$

where

- h_1 is the height of the transmitter antenna in meters,
- h_2 is the height of the receiver antenna in meters, and
- d is the link distance in meters.

Figure 8 indicates the propagation path loss for Two-Ray model at different transmitter antenna heights, h_1 , and receiver antenna height, h_2 , held constant at two (2) meters.

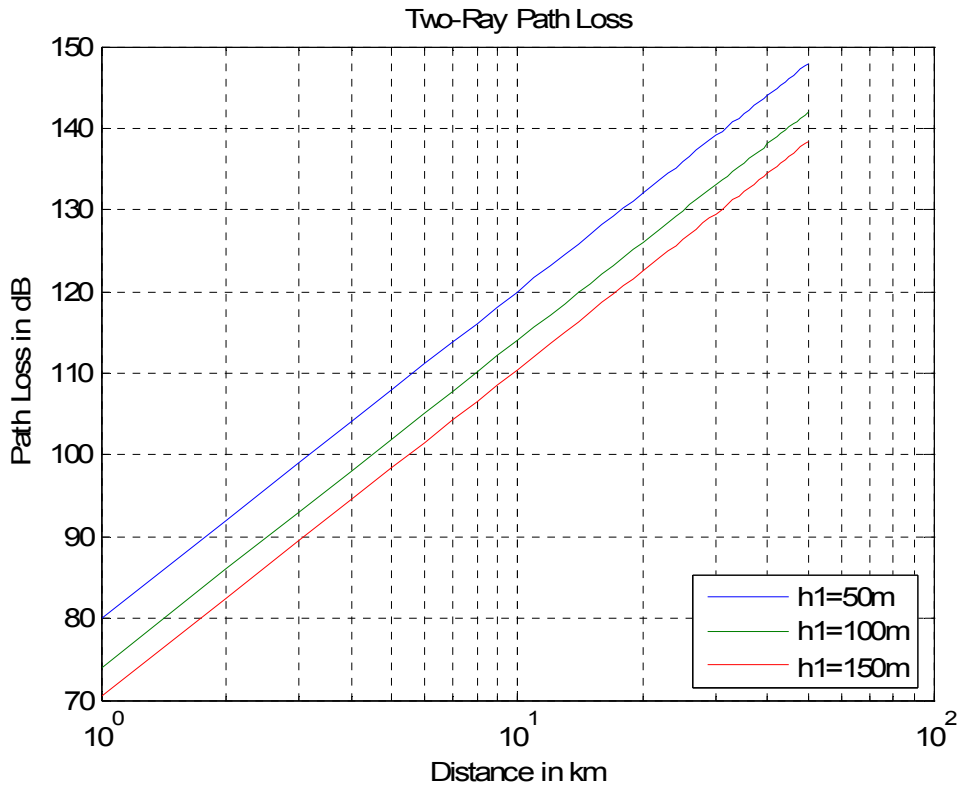


Figure 8. Two-Ray Propagation Path Loss

The key point to this approximation is that for propagation close to earth's surface, the received signal power decays inversely as the 4th power of the T-R distance or simply called the pathloss exponent.

3. Okumura-Hata Empirical Formula

Propagation in urban and suburban areas is different from the two-ray model in that a single specular ground reflection exists. Several empirical models have been developed that are based on measured data and use curve-fit equations to model propagation in areas definable urbanization. A more generalized and hence more commonly used empirical model is that of the Okumura-Hata formula. This empirical formula has been produced by Hata based on the measurements made by Okumura in the Tokyo suburbs.

Okumura's model is wholly based on measured data and does not provide any analytical explanations. It is inconvenient to use, and formulas have been devised to fit

the Okumura curves. Hata prepared a simple formula representation of Okumura's measurements in the following form [5]:

$$\bullet \quad L_{Hata} = A + B \log_{10}(d) \quad \text{for urban areas ,} \quad (2.7)$$

$$\bullet \quad L_{Hata} = A + B \log_{10}(d) - C \quad \text{for suburban areas , and} \quad (2.8)$$

$$\bullet \quad L_{Hata} = A + B \log_{10}(d) - D \quad \text{for open areas ,} \quad (2.9)$$

where

$$A = 69.55 + 26.16 \log_{10}(f) - 13.82 \log_{10}(h_b) - a(h_m) , \quad (2.10)$$

$$B = 44.9 - 6.55 \log_{10}(h_b) , \quad (2.11)$$

$$C = 5.4 + 2 \log_{10}\left(\frac{f}{28}\right) , \text{ and} \quad (2.12)$$

$$D = 40.94 + 4.78 \log_{10}(f)^2 - 19.33 \log_{10}(f) . \quad (2.13)$$

The correction factor $a(h_m)$ is defined as follows:

- for Medium or small sized cities:

$$a(h_m) = 1.1 \log_{10}(f - 0.7) h_m - 1.56 \log_{10}(f - 0.8) \text{ dB} \quad (2.14)$$

where $1\text{m} \leq h_m \leq 10\text{ m}$

- for large sized cities:

$$a(h_m) = 8.29 \log_{10}(1.54 h_m) - 1.1 \text{ dB} \quad \text{if } f \leq 200\text{MHz} \quad (2.15)$$

or

$$a(h_m) = 3.2 \log_{10}(11.75 h_m) - 4.97 \text{ dB} \quad \text{if } f > 400\text{MHz} . \quad (2.16)$$

These formulas include the following parameters:

- f : frequency (in MHz) between 150 and 1,500 MHz,
- h_b : height (in meters) of the base station, between 30 and 300 m,
- h_m : height (in meters) of the mobile station, between 1 and 20 m, and
- d : base station-mobile station distance (in km), between 1 and 20 km.

The basic principle of the Okumura-Hata formula and its variants first consists of calculating the free-space path loss. An attenuation factor is then added to this

component. Figure 9 describes the propagation path loss using the Okumura-Hata model at different sites with $h_b=50$ m, $h_m=2$ m, and $f=1$ GHz.

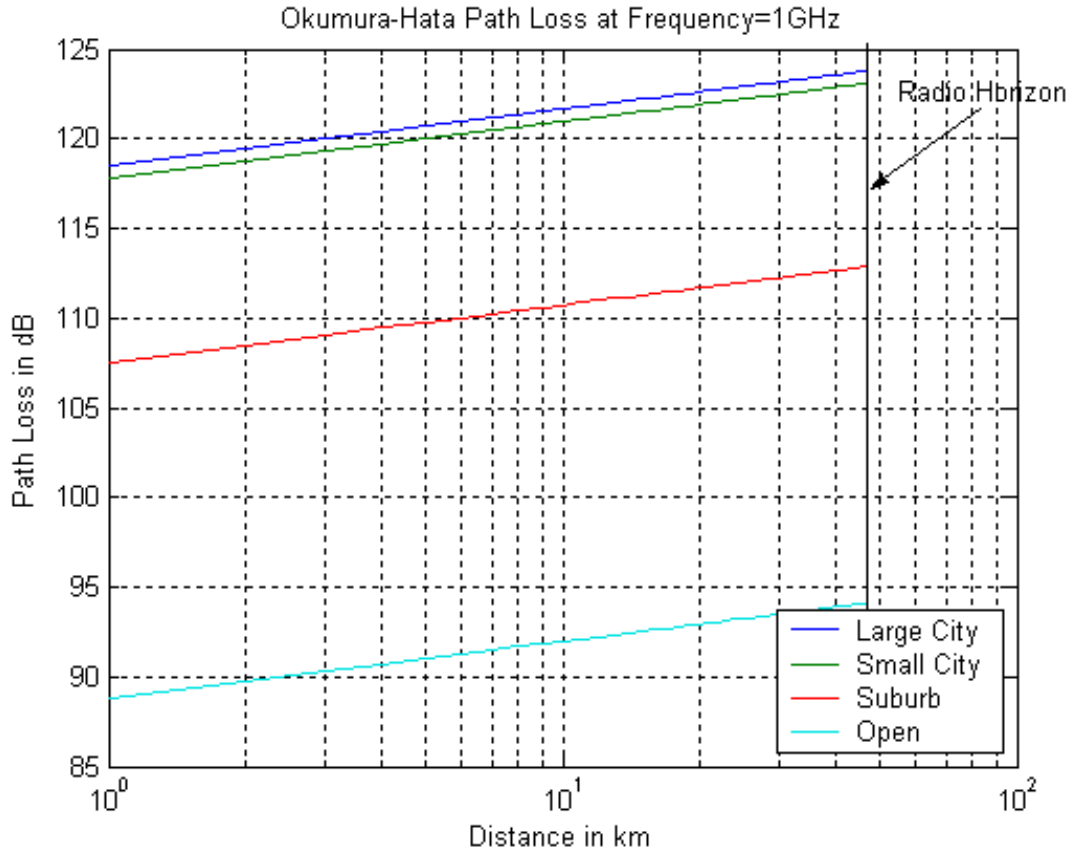


Figure 9. Okumura-Hata Propagation Path Loss

In summary, the appropriate model to use for each situation can be made by calculating the Fresnel Zone (FZ), as shown in Figure 10. If the distance between the transmitter and the receiver is less than FZ, use the free-space propagation model. If the distance between the transmitter and the receiver is greater than FZ, use the two-ray propagation model. . If the distance between the transmitter and the receiver distance is equal to FZ, the two models give the same propagation loss. For urbanized environments, use Okumura-Hata empirical formula especially when the height of the antenna is relatively low.

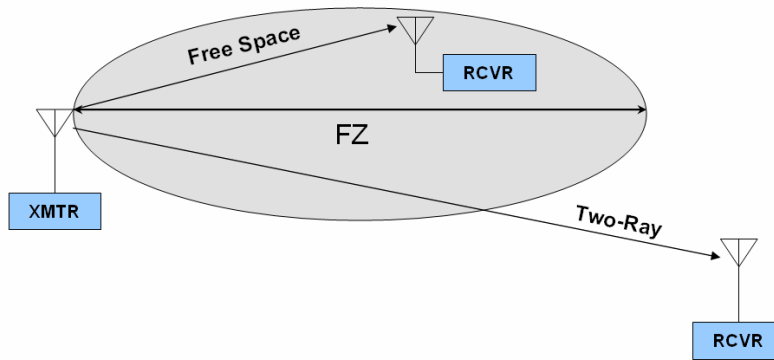


Figure 10. Fresnel Zone (FZ) (After Ref. [4].)

The formula for calculating the Fresnel zone distance is [4]

$$FZ = \frac{4\pi h_t h_r}{\lambda} \quad (2.17)$$

where

- FZ is Fresnel Zone distance in meters,
- h_t is the the height of the transmitter in meters,
- h_r is the the height of the transmitter in meters and
- λ is the wavelength of the transmitted of the transmitted signal in meters.

Alternatively, FZ can be determined by [4]

$$FZ = \frac{h_t h_r f}{24,000} \quad (2.18)$$

where FZ is in kilometers, the antenna heights are in meters, and f is the frequency in Megahertz.

THIS PAGE INTENTIONALLY LEFT BLANK

III. RECEIVER INPUT SIGNAL-TO-NOISE RATIO (SNR_{IN})

A. RECEIVED INPUT SIGNAL POWER

This analysis begins by first developing the relationship between transmitted and received powers, assuming that the radiator is isotropic and transmits uniformly in all directions. The power density at a distance from the transmitter is related to the transmitted power by the following expression [7]

$$p(d) = \frac{P_t}{4\pi d^2} \quad (3.1)$$

where

- $p(d)$ = power density in watts per sq. meters,
- P_t = transmitted power in watts, and
- d = distance in meters.

For a distance much greater than the propagation wavelength (known as the far field region), the power extracted at the receiver antenna is given as

$$P_r = \frac{P_t A_{er}}{4\pi d^2} \quad (3.2)$$

where

- P_r = received power in watts, and
- A_{er} = cross section (effective area) of the receiving antenna in sq. meters.

The antenna directivity, or the directive gain of an antenna, is the parameter that relates the power output (or input) of a real antenna to that of an ideal isotropic antenna as a purely geometric ratio. The effective radiated power (EIRP) by an antenna with respect to an isotropic radiator can be defined as

$$EIRP = P_t G_t \quad (3.3)$$

where G_t is the directive gain of transmitting antenna.

For the more general case in which the transmitter has some antenna gain relative to an isotropic antenna, the transmitted power is replaced with EIRP in the expression for received power in (3.2) to yield

$$P_r = \frac{EIRP A_{er}}{4\pi d^2}. \quad (3.4)$$

The relationship between directive gain and effective area of antenna is given as

$$G = \frac{4\pi A_e}{\lambda^2} \quad (\text{for } A_e \gg \lambda^2) \quad (3.5)$$

where λ is the wavelength in meters.

Therefore, the received power can also be written as

$$P_r = \frac{EIRP G_r}{(4\pi d/\lambda)^2} \quad (3.6)$$

where G_r is the directive gain of the receiving antenna or

$$P_r = \frac{EIRP G_r}{L_s} \quad (3.7)$$

where L_s is the collection of terms $(4\pi d/\lambda)^2$ and is called path loss or free space loss.

Generally, the path loss is specific for a given scenario (site-specific). Two commonly used models are the free space model and the two-ray path model, described earlier.

B. RECEIVER INPUT NOISE POWER

The noise which the signal competes with is usually generated within the receiver itself. If the receiver operated in a perfectly noise free environment so that no external sources of noise accompany the signal, there would still be noise generated in the receiver due to thermal effects, called thermal noise. Its magnitude is directly proportional to the bandwidth and the absolute temperature. The thermal noise power (noise floor) generated at the input of a receiver is given as [8]

$$P_{th} = kTB_n \quad (3.8)$$

where

- P_{th} = Thermal noise power in watts,
- k = Boltzmann's constant (1.38×10^{-23} J/Kelvin),
- T = system temperature in degrees Kelvin, and
- B_n = noise bandwidth in Hertz.

The noise bandwidth mentioned here is not the same as the more familiar half-power bandwidth, though the half-power bandwidth is often used as a reasonable approximation for noise bandwidth.

The system noise temperature (T), in equation 3.8, is defined as the effective noise temperature of the receiver, including the effects of antenna temperature, and is expressed as [8]

$$T = T_a + T_e \quad (3.9)$$

where

- T_a = antenna temperature, and
- T_e = receiver effective noise temperature.

Noise Figure, which is the parameter that relates the signal-to-noise ratio at the input of a receiver to the signal-to-noise ratio at the output, will be described. The noise figure which indicates the degradation caused by the receiver is described as [7]

$$F = \frac{SNR_{in}}{SNR_{out}} = \frac{S_{in}/N_{in}}{GS_{in}/G(N_{in} + N_r)} \quad (3.10)$$

where

- S_{in} = signal power at the input,
- N_{in} = noise power at the input,
- N_r = receiver noise, and
- G = receiver gain.

The above equation can be simplified to

$$F = \frac{(N_{in} + N_r)}{N_{in}} = 1 + \frac{N_r}{N_{in}}. \quad (3.11)$$

Rearranging this equation,

$$N_r = (F - 1)N_{in}. \quad (3.12)$$

In equation 3.12, N_r can be replaced with $kT_e B_n$ and N_{in} with $kT_o B_n$ giving

$$kT_e B_n = (F - 1)kT_o B_n \quad (3.13)$$

or

$$T_e = (F - 1)T_o \quad (3.14)$$

where T_o is the standard temperature of 290°K.

The system noise temperature described in equation 3.9 can therefore be given as

$$T = T_a + (F - 1) T_o . \quad (3.15)$$

The thermal noise power described in equation 3.8 is therefore expressed as

$$P = k [T_a + (F - 1)T_o] B_n . \quad (3.16)$$

C. INPUT SIGNAL-TO-NOISE RATIO

The signal-to-noise ratio at the input of the receiver can now be expressed using the signal and noise power expressions described above as

$$SNR_{in} = \frac{\text{received power}}{\text{noise power}} = \frac{P_t G_t G_r / L_s}{k T_s B_n} \quad (3.17)$$

or

$$SNR_{in} = \frac{P_t G_t G_r}{L_s k T_s B_n} . \quad (3.18)$$

Based on the above discussion, the signal-to-noise ratio at the input of the receiver is described in Figure 11 through Figure 13 for the free space model and in Figure 14 through Figure 16 for the two-ray model. Considering a frequency modulated signal with the following parameters:

- Transmitter Power = 100 watts,
- Transmitter Gain = 5 dB,
- Receiver Gain = 2 dB,
- Frequency = 30 MHz,
- Transmitter Antenna Height = 10 m,
- Receiver Antenna Height = 2 m,
- Receiver Noise Figure = 4,
- Antenna Temperature = 290° K, and
- Bandwidth = 10 KHz.

The SNR variations at the input of the receiver for a free space propagation model with changing transmitted powers and keeping all the remaining parameters mentioned above as constant, can be observed from Figure 11.

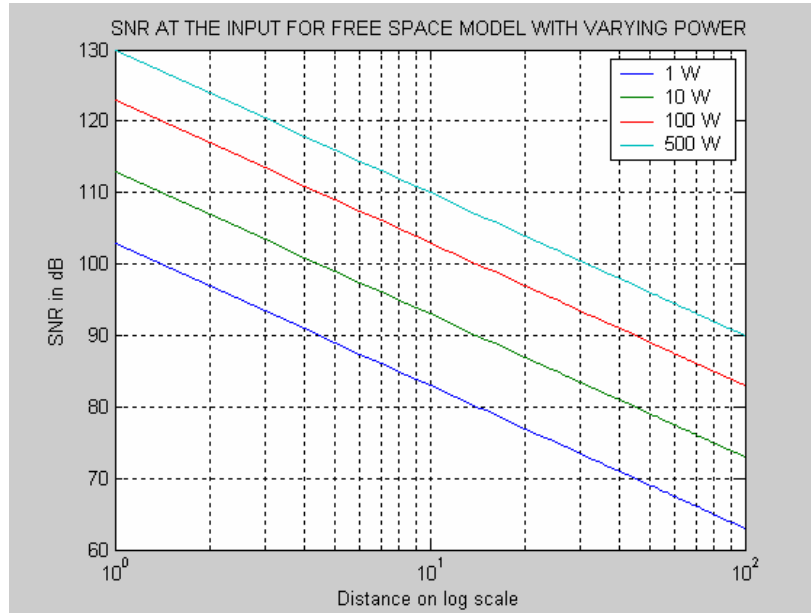


Figure 11. SNR at the Input for Free Space Model with Varying Power

Similarly, the SNR variations with change in transmitted frequencies, while keeping all the other parameters constant, can be observed from Figure 12.

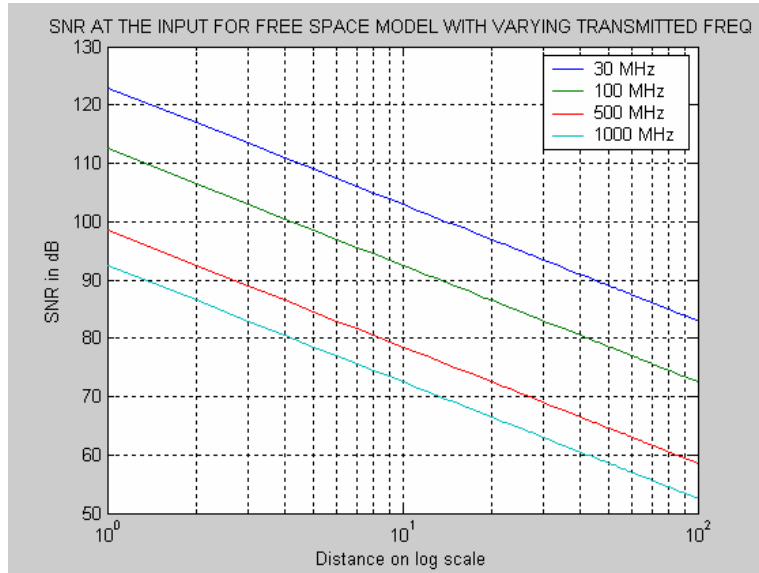


Figure 12. SNR at the Input for Free Space Model with Varying Transmitted Frequency

Again, for a free space propagation model, the change in SNR with respect to changing transmitting antenna gain and remaining parameters being kept constant is plotted in Figure 13.

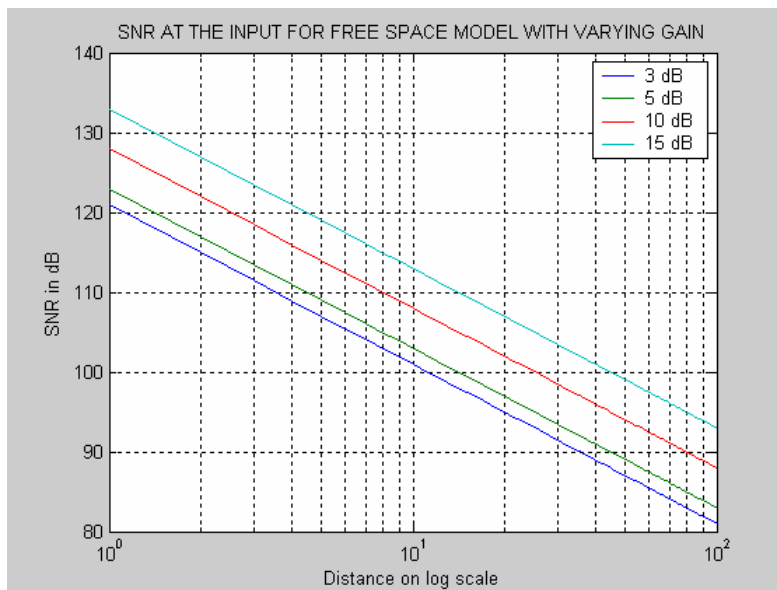


Figure 13. SNR at the Input for Free Space Model with Varying Gain

For the two-ray propagation model, the SNR dependence on transmitted power, with all other parameters being constant, can be observed from Figure 14.

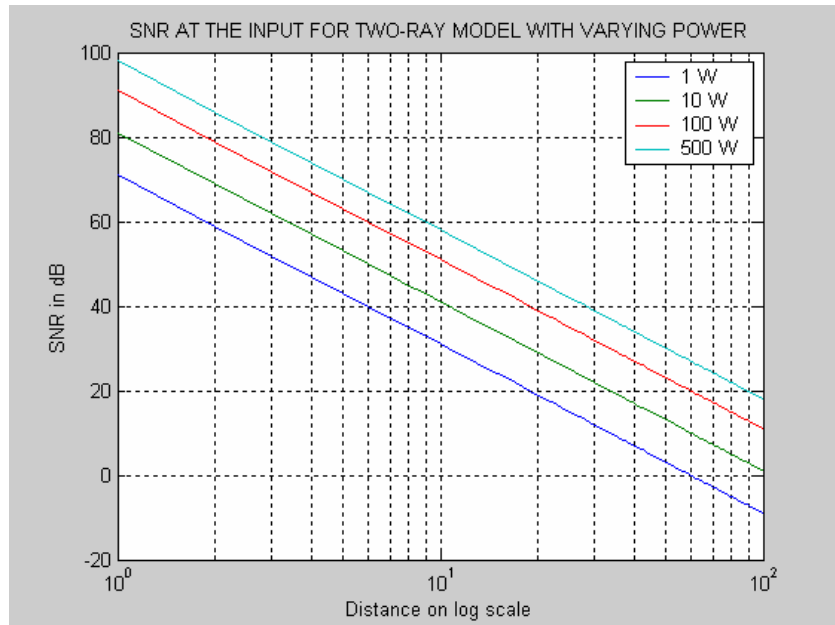


Figure 14. SNR at the Input for Two Ray Model with Varying Power

Similarly, SNR with respect to changing antenna gain and other parameters being constant is plotted for two ray propagation model in Figure 15.

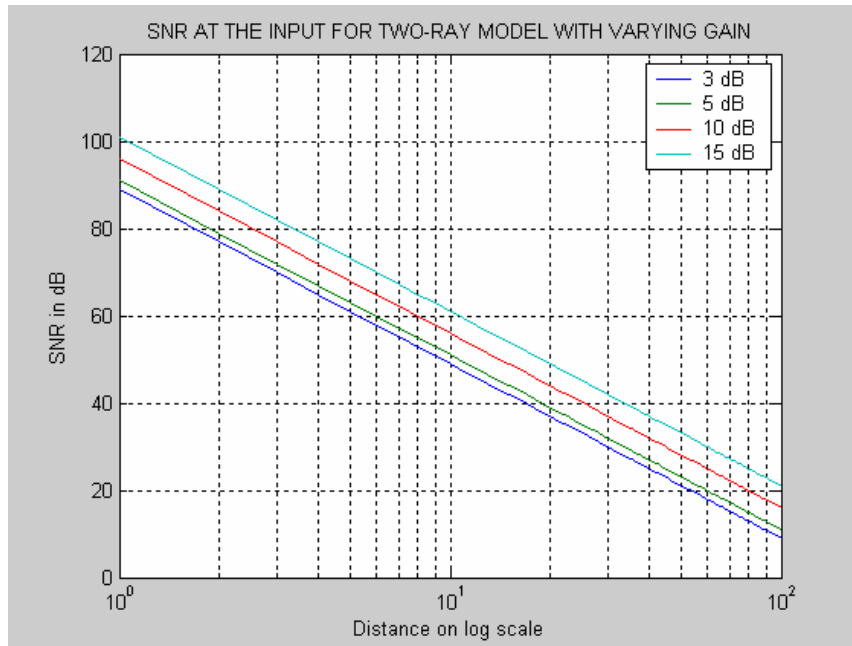


Figure 15. SNR at the Input for Two Ray Model with Varying Gain

Again for the two-ray propagation model, the change in SNR with respect to changing antenna height while other parameters being kept constant is plotted in Figure 16.

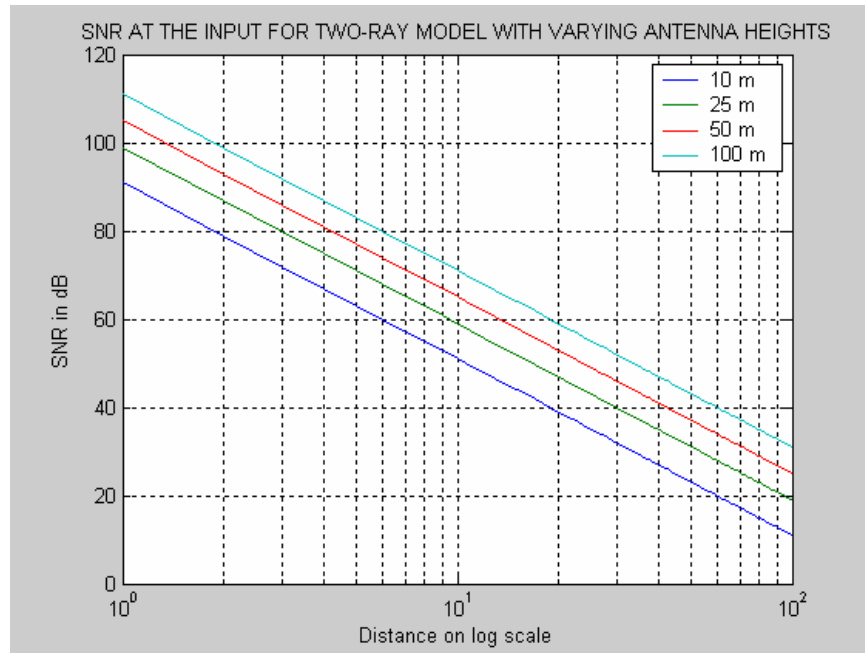


Figure 16. SNR at the Input for Two Ray Model with Varying Antenna Heights

IV. RECEIVER OUTPUT SIGNAL-TO-NOISE RATIO (SNROUT)

The signal-to-noise ratio at the receiver output is an important parameter because it indicates the quality of the output signal. It is defined as the ratio of the average power of the demodulated message signal to the average power of the noise, both measured at the receiver output [9]. This analysis will be performed under the following analog conditions:

- Amplitude Modulation Coherent Detection,
- Amplitude Modulation Non-coherent Detection, and
- Frequency Modulation.

A. AMPLITUDE MODULATION – COHERENT DETECTION

The analysis in this section deals with synchronous (coherent) demodulation of signals at the receiver. In order to demodulate a signal coherently, the local oscillators of both the receiver and the transmitter need to be synchronized in frequency and phase [9]. Furthermore, the noise in this analysis is assumed to be additive, white and Gaussian. Three different types of AM systems are considered

- Double-Sideband Suppressed Carrier (DSB-SC),
- Single-Sideband Suppressed Carrier (SSB-SC), and
- Double-Sideband Large Carrier (DSB-LC or AM).

Although the AM signal is usually demodulated non-coherently, in this research, coherent detection is considered for comparison with other systems. The block diagram applicable to all amplitude modulation types mentioned above for coherent demodulation is shown in Figure 17.

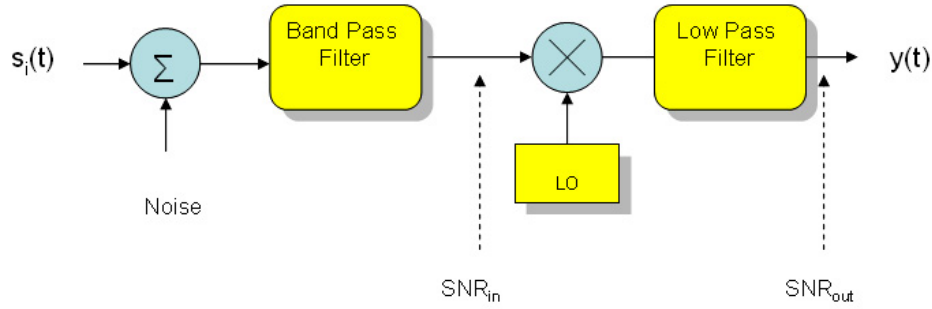


Figure 17. Block Diagram for Coherent Demodulation

Noise and signal at the input of the demodulator are first analyzed and expressions for their average powers are described. Assuming noise to be white Gaussian, the noise power at the input is [10]

$$N_{in} = N_o B \quad \text{for SSB} \quad (4.1)$$

and

$$N_{in} = 2N_o B \quad \text{for AM and DSB-SC,} \quad (4.2)$$

where

- N_o = average noise power per unit bandwidth, and
- B = noise bandwidth.

The SSB, DSB-SC and AM signals at the input of the demodulator are summarized as

$$s_{SSB}(t) = [f(t) \cos(\omega_o t + \theta)] \pm [f(\hat{t}) \sin(\omega_o t + \theta)], \quad (4.3)$$

$$s_{DSB}(t) = f(t) \cos(\omega_o t + \theta), \quad (4.4)$$

$$s_{AM}(t) = [A_c + f(t)] \cos(\omega_o t + \theta), \quad (4.5)$$

where

- $f(t)$ = information signal,
- $f(\hat{t})$ = Hilbert Transform of $f(t)$, and
- A_c = carrier amplitude.

The average powers of the above mentioned input signals are

$$S_i = \overline{f^2(t)} \quad \text{for SSB,} \quad (4.6)$$

$$S_i = \overline{f^2(t)}/2 \quad \text{for DSB, and} \quad (4.7)$$

$$S_i = \left[A_c^2 + \overline{f^2(t)} \right] / 2 \quad \text{for AM.} \quad (4.8)$$

The above signal and noise powers are now used to describe the signal-to-noise ratio at the input of the demodulator for SSB, DSB-LC and AM systems as

$$SNR_{in} = \frac{\overline{f^2(t)}}{N_o B} \quad \text{for SSB,} \quad (4.9)$$

$$SNR_{in} = \frac{\overline{f^2(t)}/2}{2N_o B} \quad \text{for DSB-SC, and} \quad (4.10)$$

$$SNR_{in} = \frac{\left[A_c^2 + \overline{f^2(t)} \right] / 2}{2N_o B} \quad \text{for AM.} \quad (4.11)$$

Now consider the signal and noise at the output of the coherent demodulator. At the output, the superposition principle is applied, that is, signal and noise components may be determined from the response of the demodulator acting separately on each component. The output signal response of a coherent demodulator is identical for SSB, DSB-SC and AM signals expressed as [10]

$$s_o(t) = f(t)/2. \quad (4.12)$$

The output signal power is therefore

$$S_{out} = \overline{f^2(t)}/4. \quad (4.13)$$

The noise at the output of the demodulator is

$$N_{out} = (N_o B)/4 \quad \text{for SSB,} \quad (4.14)$$

and

$$N_{out} = (N_o B)/2 \quad \text{for AM and DSB-SC.} \quad (4.15)$$

The signal-to-noise ratio at the output of the demodulator can now be described by the above mentioned signal and noise expressions for SSB, DSB-SC and AM systems as

$$SNR_{out} = \frac{\overline{f^2(t)}/4}{(N_o \times B)/4} = \frac{\overline{f^2(t)}}{(N_o \times B)} \quad \text{for SSB,} \quad (4.16)$$

$$SNR_{out} = \frac{\overline{f^2(t)}/4}{(N_o \times B)/2} = \frac{\overline{f^2(t)}}{2 \times (N_o \times B)} \quad \text{for DSB-SC, and} \quad (4.17)$$

$$SNR_{out} = \frac{\overline{f^2(t)}/4}{(N_o \times B)/2} = \frac{\overline{f^2(t)}}{2 \times (N_o \times B)} \quad \text{for AM.} \quad (4.18)$$

These expressions of SNR are also used to express the SNR at the output in terms of SNR at the input of the demodulator as [10]

$$SNR_{out} = SNR_{in} \quad \text{for SSB,} \quad (4.19)$$

$$SNR_{out} = 2 SNR_{in} \quad \text{for DSB-SC, and} \quad (4.20)$$

$$SNR_{out} = 2 \frac{\overline{f^2(t)}}{[A_c^2 + \overline{f^2(t)}]} SNR_{in} \quad \text{for AM.} \quad (4.21)$$

B. AMPLITUDE MODULATION – NON-COHERENT DETECTION

As mentioned earlier, AM signal is typically detected non-coherently using an envelope detector or a square-law detector. Non-coherent detection is a non-linear process. A consequence of this non-linearity is the onset of threshold, with distinctly different detector performance for the input SNR above and below the threshold. This subject is analyzed below. Two different types of systems, Double-Sideband Large Carrier and Vestigial Sideband Large Carrier, are considered for the non-coherent analysis.

Moreover, in calculations for the analysis, either the signal-to-noise ratio (SNR) or the carrier-to-noise ratio (CNR) at the receiver input may be used and this SNR-CNR relationship is described first.

The Carrier-to-Noise Ratio (CNR) at the receiver input is

$$CNR_{in} = \frac{P_c}{N_{in}}, \quad (4.22)$$

where P_c is the carrier power.

The average power in the carrier of an AM signal is given as

$$P_c = A_c^2/2, \quad (4.23)$$

and the noise power as described in equation 3.8.

Therefore, the carrier-to-noise ratio is

$$CNR_{in} = \frac{\frac{A_c^2}{2}}{kT_s B}. \quad (4.24)$$

The average power of AM signal at the input as described in equation 4.8 can also be written as

$$\begin{aligned} P &= \frac{[A_c^2 + \overline{A_m^2}]}{2}, \\ &= \left[A_c^2 \left\{ 1 + (\overline{A_m}/A_c)^2 \right\} \right] / 2, \text{ or} \\ &= \left[A_c^2 (1 + \overline{m^2}) \right] / 2, \end{aligned} \quad (4.25)$$

where

- A_m = Modulating signal amplitude and the over bar indicates the average value, and
- m = average power of the normalized modulating signal.

Therefore, signal-to-noise ratio is

$$SNR_{in} = \frac{[A_c^2 (1 + \overline{m^2})] / 2}{kT_s B}, \quad (4.26)$$

or in terms of carrier-to-noise ratio

$$SNR_{in} = (1 + \overline{m^2}) CNR_{in}. \quad (4.27)$$

1. Double-Sideband Large Carrier (DSB-LC or AM)

The Amplitude Modulation system will be analyzed for Envelope and Square Law detection.

a. Envelope Amplitude Modulation Detection

The most common demodulation method of AM is by using an envelope detector in the receiver as shown in Figure 18.

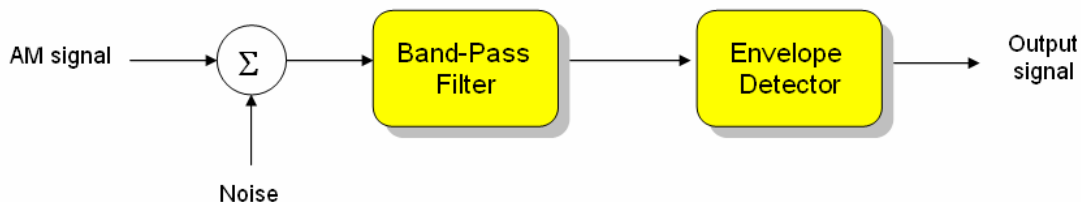


Figure 18. Block Diagram for Envelope AM Detection

Since the band-pass filter bandwidth is twice the information signal bandwidth, the signal power and the noise power at the envelope detector input are the same as at the input to the demodulator of the coherent detector analyzed earlier and described in equations 4.8 & 3.8 respectively [10].

Now the signal and noise powers at the output are determined by the response of the envelope detector. Assuming the envelope detector to be linear, the output signal and noise are described for low-noise and low-signal cases.

(1) Low-Noise Case

If the magnitude of the input signal is large in relation to the input noise magnitude, then the signal and noise powers at the output of the detector are [10]

$$S_{out} = \overline{f^2(t)}, \text{ and} \quad (4.28)$$

$$N_{out} = kT_s B_n. \quad (4.29)$$

From the ratios of signal-to-noise at the output and input of the envelope detector

$$SNR_{out} = 2 \frac{\overline{f^2(t)}}{\left[A_c^2 + \overline{f^2(t)} \right]} SNR_{in}, \quad (4.30)$$

$$SNR_{out} = 2 \frac{\left(\overline{A_m}/A_c\right)^2}{\left[1 + \left(\overline{A_m}/A_c\right)^2\right]} SNR_{in}, \quad (4.31)$$

or

$$SNR_{out} = 2 \frac{\overline{m^2}}{\left[1 + \overline{m^2}\right]} SNR_{in} \quad \text{for } CNR_{in} \gg 1. \quad (4.32)$$

The SNR at the output in terms of CNR therefore is

$$SNR_{out} = 2 \overline{m^2} CNR_{in} \quad \text{for } CNR_{in} \gg 1. \quad (4.33)$$

(2) Low-Signal Case

If the signal magnitude is low compared to the noise magnitude, then the SNR_{out} can be approximated as

$$SNR_{out} \approx 2 \frac{\overline{m^2}}{\left[1 + \overline{m^2}\right]} SNR_{in} \frac{(1.85 SNR_{in})}{\left[1 + \overline{m^2}\right]}. \quad (4.34)$$

For the case of 100% modulation, the above expression is [3]

$$SNR_{out} \approx 0.925 SNR_{in}^2 \quad \text{for } CNR_{in} \ll 1. \quad (4.35)$$

The inspection of the above two cases indicates that there is some value of SNR_{in} below which the output SNR degrades much more rapidly than above such values [11]. The same effect can be observed in Figure 19.

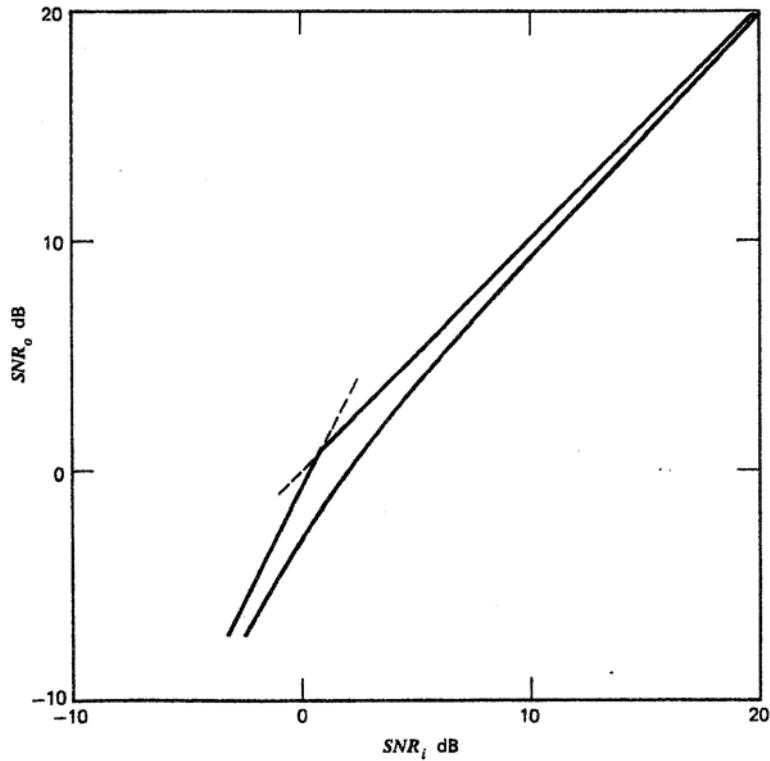


Figure 19. Envelope Detection Plot (From Ref. [11].)

The transition of behavior is usually called the Threshold Effect and the value of SNR_{in} at the transition point is called the Threshold Signal-to-Noise Ratio. The exact expression for the region around the threshold is not available in closed form. However, this transition is not abrupt and can be observed in Figure 19.

b. Square-Law Amplitude Modulation Detection

For AM detection using full-wave square-law rectification, the results of the previous section do not apply [11]. The SNR characteristics for square-law detection are discussed below. As for envelop detection, the output signal and noise are described for low-noise and low-signal cases.

(1) Low-Noise Case

For low noise case, that is, large carrier-to-noise ratio, the signal-to-noise ratio at the output is approximated as [11]

$$SNR_{out} \approx 2 \overline{m^2} CNR_{in} \quad CNR_{in} \gg 1, \quad (4.36)$$

or in terms of signal-to-noise ratio, as

$$SNR_{out} \approx 2 \frac{\overline{m^2}}{[1 + \overline{m^2}]} SNR_{in}. \quad (4.37)$$

(2) Low-Signal Case

For low signal case, that is, low carrier-to-noise ratio, the approximation is [11]

$$SNR_{out} \approx 8/3 \overline{m^2} CNR_{in}^2 \quad \text{for } CNR_{in} \ll 1, \quad (4.38)$$

or

$$SNR_{out} \approx 8/3 \frac{\overline{m^2}}{(1 + \overline{m^2})^2} SNR_{in}^2. \quad (4.39)$$

The plot of signal-to-noise ratio at the output as a function of signal-to-noise ratio at the input for the square law detector is given in Figure 20. Similar to the envelope detector case, the threshold effect produced by the non-linear devices can be observed.

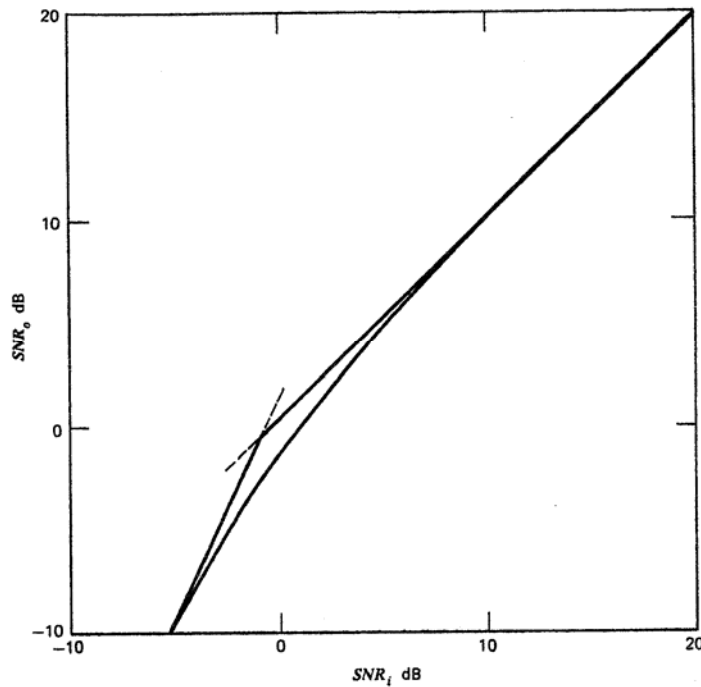


Figure 20. Square Law Detection Plot (From Ref. [11].)

2. Vestigial Sideband Large Carrier (VSB-LC)

When removing the unwanted sideband from a DSB signal, a portion of the sideband remains because of practical limitations of the filter. A practical filter can only remove the sideband partially, thus producing an asymmetric sideband. This gives rise to the term “vestige.” This asymmetric sideband results in a spectrum of VSB of about 125 percent of SSB and about 62 percent of DSB rather than 50 percent due to the imperfection [11].

VSB modulation is employed in television transmission; therefore, the demodulation technique is influenced by the requirement of the receiver to be simple and inexpensive [9]. An envelope or square-law detection technique is therefore used for the demodulation but this necessitates the addition of a carrier to the VSB signal. The insertion of a carrier allows the VSB modulated signal to be demodulated non-coherently with the bandwidth requirement being the only difference between VSB and AM.

The performance of the envelope and square-law detectors used for VSB demodulation is similar to the performance of the same detector for AM after accounting for input bandwidth differences. The receiver bandwidth for the AM signal is twice the information bandwidth, whereas the receiver bandwidth for VSB is, in general, $1+\xi$, with the value of ξ being less than one. Therefore, the noise power within the receiver bandwidth is lower for VSB by a factor of $(1+\xi)/2$.

The expression for AM detector performance thus could also be used for VSB, but with the SNR at the input multiplied by $2/(1+\xi)$. The signal-to-noise ratio is therefore be analyzed for Envelope and Square Law detection.

a. Envelope VSB-LC Detection

For AM detection, the output signal and noise is described for two different cases.

(1) Low-Noise Case

$$SNR_{out} = \frac{4}{(1+\xi)} \frac{\overline{m^2}}{[1+\overline{m^2}]} SNR_{in} \quad \text{for } CNR_{in} \gg 1. \quad (4.40)$$

The SNR at the output can also be described in terms of CNR as

$$SNR_{out} = \overline{m^2} \frac{4}{(1+\xi)} CNR_{in} \quad \text{for } CNR_{in} \gg 1. \quad (4.41)$$

(2) Low-Signal Case

If the signal magnitude is low as compared to the noise magnitude, then the SNR_{out} can be approximated as

$$SNR_{out} \approx 4 \frac{2^2}{(1+\xi)^2} \frac{\overline{m^2}}{[1+\overline{m^2}]} SNR_{in} \frac{(1.85 \times SNR_{in})}{[1+\overline{m^2}]}. \quad (4.42)$$

b. Square-Law VSB-LC Detection

Again, using the analysis of AM square-law demodulation, the output signal-to-noise ratio for VSB-LC for low-noise and low-signal cases is described.

(1) Low-Noise Case

For the low noise case, that is, large carrier-to-noise ratio, the signal-to-noise ratio at the output can be approximated as

$$SNR_{out} \approx \frac{4}{(1+\xi)} \overline{m^2} CNR_{in} \quad \text{for } CNR_{in} \gg 1, \quad (4.43)$$

or in terms of signal-to-noise ratio

$$SNR_{out} \approx \frac{4}{(1+\xi)} \frac{\overline{m^2}}{[1+\overline{m^2}]} SNR_{in}. \quad (4.44)$$

(2) Low-Signal Case

For the low signal case, that is, low carrier-to-noise ratio, the approximation is

$$SNR_{out} \approx 8/3 \frac{2^2}{(1+\xi)^2} \overline{m^2} CNR_{in}^2 \quad \text{for } CNR_{in} \ll 1, \quad (4.45)$$

or

$$SNR_{out} \approx 8/3 \frac{2^2}{(1+\xi)^2} \frac{\overline{m^2}}{(1+\overline{m^2})^2} SNR_{in}^2. \quad (4.46)$$

C. FREQUENCY MODULATION

1. Basic Principles

Frequency Modulation (FM) is a form of modulation that represents information as variations in the instantaneous frequency of a carrier wave. (Contrast this with amplitude modulation, in which the amplitude of the carrier is varied while its frequency remains constant.) It is a nonlinear process in which the frequency of the carrier is varied according to the message signal.

Frequency modulation requires a wider bandwidth than amplitude modulation by an equivalent modulating signal, but this also makes the signal more robust against interference. Frequency modulation is also more robust against simple signal amplitude fading phenomena. Figure 21 is an illustrative FM waveform [12]:

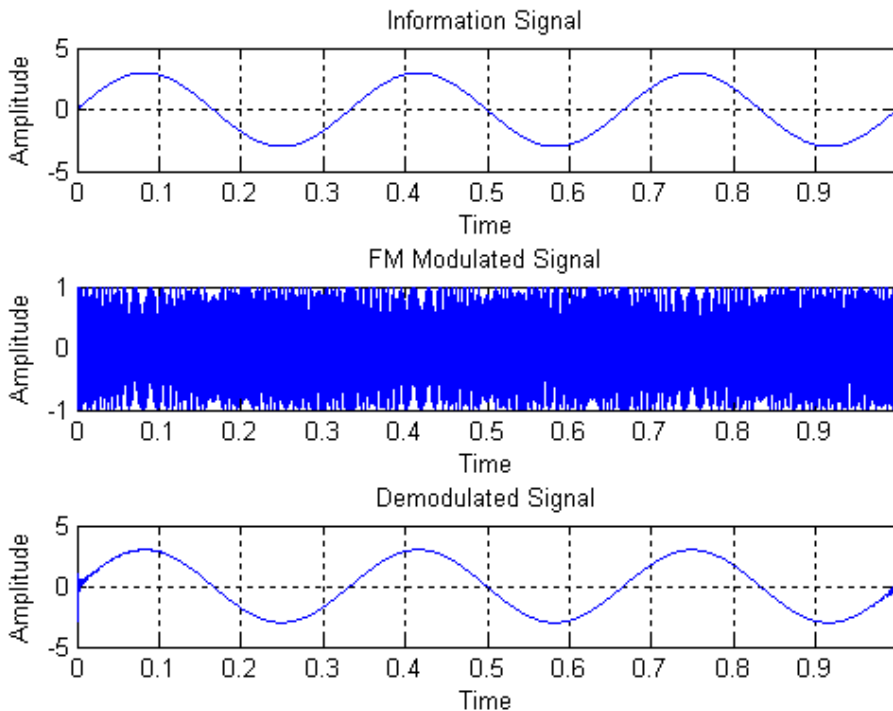


Figure 21. Illustrative FM Waveform

2. Transmission Bandwidth

For an arbitrary modulating signal $m(t)$, the bandwidth is virtually impossible to determine exactly. For sinusoidal modulation, the bandwidth, B , is theoretically infinite, but for practical purposes, it is calculated using *Carson's Formula* as [13]

$$B = 2(\beta + 1)f_m \quad (4.47)$$

where B is the bandwidth, β denotes the modulation index and f_m is the highest frequency component of the modulating signal.

The signal-to-noise ratio at the receiver input is calculated as

$$SNR_{in} = \frac{P_t G_t G_r}{L_p k T_s B_r} = \frac{P_t G_t G_r}{L_p k T_s (2(\beta + 1)f_m)}. \quad (4.48)$$

3. Frequency Modulation Detection

FM detection is a non-linear process. A consequence of the non-linearity is the onset of an input signal-to-noise ratio threshold that delineates the FM detector performance. The threshold is typically in the range of 10 to 13 dB. For an arbitrary modulating signal, a closed-form expression exists for FM detector performance for the low-noise case (input SNR well above threshold). For the case of arbitrary input SNR (around and below threshold) the closed form expression exists only for the case of a sinusoidal modulating signal. The expressions to follow apply to both narrowband ($\beta < 0.5$) and wideband FM ($\beta > 0.5$).

4. Input SNR above Threshold

The output SNR for a given input SNR and an arbitrary modulating signal $m(t)$ is given by [14]

$$SNR_{out} = 6\beta^2(\beta + 1) \left(\frac{m}{m_{peak}} \right)^2 SNR_{in} \quad (4.49)$$

where β is the modulation index and m_{peak} is the peak value of the arbitrary modulating signal and the over-bar denotes averaging.

In case of a sinusoidal modulating signal, the average value is $\frac{1}{2}$ and the above expression becomes

$$SNR_{out} = 3\beta^2(\beta + 1)SNR_{in} \quad (4.50)$$

or in terms of Carrier to Noise Ratio(CNR) [14, 15]

$$SNR_{out} = \frac{3}{2}\beta^2 CNR . \quad (4.51)$$

By inspection, these results seem to indicate that the performance of the FM systems can be increased without limit simply by increasing the modulation index, β . However, as β increases, the transmission bandwidth increases, and consequently, SNR_{in} decreases. These equations for SNR_{out} are valid only when $SNR_{in} \gg 1$ (i.e. input signal power is above the threshold), so SNR_{out} does not increase to an excessively large value simply by increasing the FM modulating index.

For the case of sinusoidal modulation, the output SNR for an FM discriminator without deemphasis is shown to be [13, 14]

$$SNR_{out} = \frac{3\beta(\beta + 1)SNR_{in}}{1 + \left[\frac{24}{\pi} \beta(\beta + 1) \right] SNR_{in} e^{-SNR_{in}}} . \quad (4.52)$$

Figure 22 is the graph showing the quieting threshold for the different modulating indices.

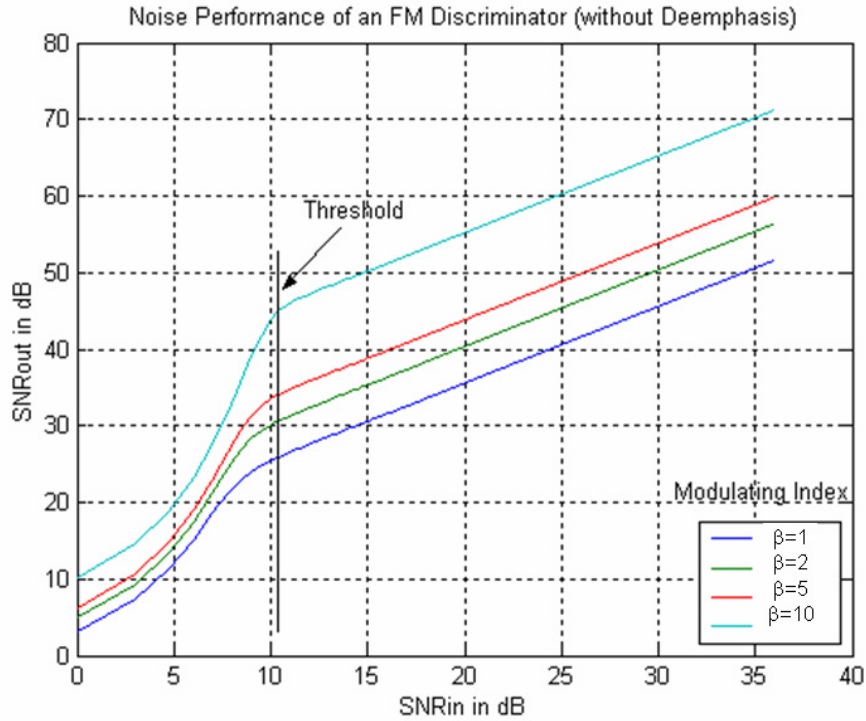


Figure 22. Quieting Threshold (After Ref. [13].)

5. Preemphasis and Deemphasis

The noise suppression ability of FM decreases as the modulating frequency increases. However, in speech and music, the higher frequency components are generally the low level components, and they are more prone to the effects of noise. To improve this situation, the high frequency components of the audio signal are boosted in amplitude relative to the lower frequency components prior to modulation. This results in greater deviation at the higher frequencies and better noise suppression. This process is known as preemphasis as illustrated in the block diagram of Figure 23 [15].

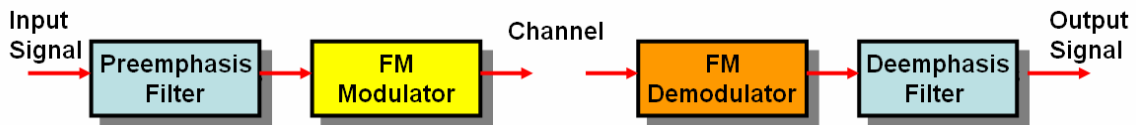


Figure 23. Preemphasis and Deemphasis Networks in FM Transmission (After Ref. [15].)

The output signal power for preemphasis-deemphasis system is the same as that when preemphasis-deemphasis is not used because the overall frequency response of the system to $m(t)$ is flat over the bandwidth of B hertz. The output SNR is given by [14]

$$SNR_{out} = 2\beta^2(\beta + 1) \left(\frac{B_m}{B_{filter}} \right)^2 \overline{\left(\frac{m}{m_{peak}} \right)^2} SNR_{in}, \quad (4.53)$$

where

- β is the FM index,
- B_m is the bandwidth of the baseband,
- B_{filter} is the 3-db bandwidth of the deemphasis filter,
- m_{peak} is the peak value of the arbitrary modulating signal $m(t)$, and
- $\overline{(m/m_{peak})^2}$ is the square of the rms value of $m(t)/m_{peak}$,

or in equivalent baseband SNR as [14]

$$SNR_{out} = \beta^2 \left(\frac{B_m}{B_{filter}} \right)^2 \overline{\left(\frac{m}{m_{peak}} \right)^2} CNR. \quad (4.54)$$

When a sinusoidal test tone is transmitted over this FM system, $\overline{(m/m_{peak})^2} = 1/2$ and output SNR becomes [14]

$$SNR_{out} = \frac{1}{2} \beta^2 \left(\frac{B_m}{B_{filter}} \right)^2. \quad (4.55)$$

6. Threshold Extension in FM

FM receiver performance deteriorates rapidly when the input SNR falls below the threshold, that is for $SNR_{in} < 10$ dB. However, there are several techniques that could lower the threshold below that provided by a receiver that uses an FM discriminator, such as FM FeedBack (FMFB) and Phase-Locked Loop (PLL) FM receivers. The expressions

presented for FM discriminators are valid for the FMFB and PLL FM receivers, but the range of validity of the expressions is extended to lower SNR_{in} . For FMFB receivers, typical threshold extensions are on the order of 5 dB (to about 5 dB). For PLL receivers, typical threshold extensions are on the order of 3 dB (to about 7 dB) [13, 14, 15].

THIS PAGE INTENTIONALLY LEFT BLANK

V. JAMMING OBJECTIVES FOR TARGETED SIGNALS

This chapter formulates the jamming objectives for targeted signals based on their capabilities and limitations.

The most uniformly effective interference used in jamming is “broadband noise” covering the acoustic range from 20 Hz to about 4 kHz. Extensive subjective tests have established statistical guidelines for SNRs required for various levels of speech intelligibility.

Word articulation expressed in percent is a quantitative measure that refers to the percentages of test words correctly identified in an intelligibility test. For example, 80% word articulation requires an SNR of +12 dB, while at SNR = 0 (equal powers of speech and noise) the word articulation is just under 40%. Speech is rendered completely unintelligible for an SNR of approximately -9 dB. This is depicted in Figure 24 [17].

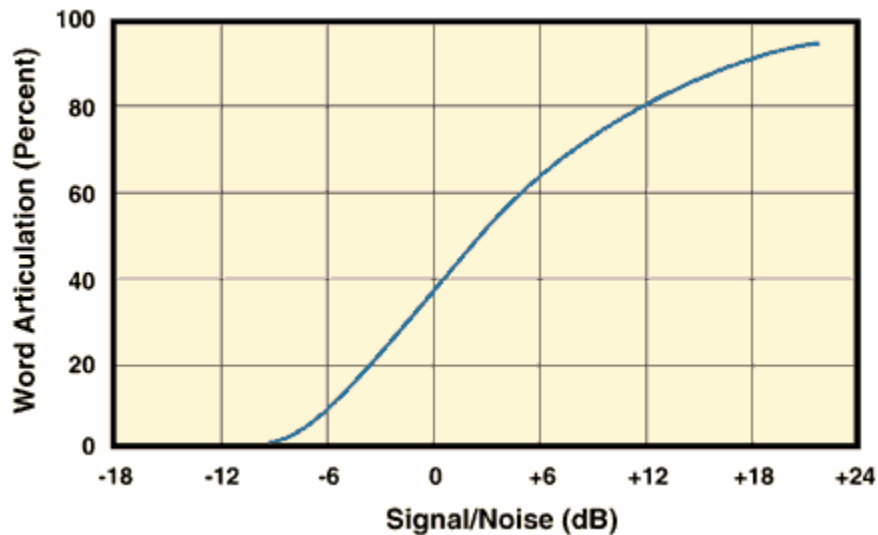


Figure 24. Effect of Broadband Masking Noise (From Ref. [12].)

Broadband noise, covering the acoustic frequency range from 20 Hz to about 4 kHz, renders speech completely unintelligible at an SNR of approximately -9 dB. Ten percent intelligibility occurs at an SNR of approximately -6 dB.

A. AMPLITUDE MODULATED (AM) BROADCAST RADIO AND BROADCAST TV

For AM radio and TV signals, the jamming objective is to create sufficiently low CJNR such that the speech or video is rendered useless to the listener and viewer. Statistical SNR thresholds have been established for speech intelligibility and image quality. Based on known demodulation properties, these SNR thresholds can be related to the CNR/CNJR at the receiver input. Because propagation renders amplitudes for the target signal and jamming signals as random variables, this will require calculating the probability that, for the given jamming scenario, the CJNR will be below the desired threshold.

B. FREQUENCY MODULATED (FM) BROADCAST RADIO

For FM radio signals, the objective is to exploit the “FM Station Capture” (FMSC) effect. FMSC refers to the fact that whenever two FM signals share the same carrier frequency, an FM receiver will lock onto the stronger signal (station) and suppress the reception of the weaker signal (station). For the weaker station to be reliably suppressed, the threshold for the FMSC is generally accepted as 3 dB.

Therefore, for FM broadcast and two-way FM radios, the objective is to create an FM jamming signal (an interfering FM “station”) that is at least 3 dB stronger at the target receiver than the FM signal being jammed. Since propagation renders signal amplitudes as random variables, this will also require determination of the probability that the FM jamming signal will exceed the FM signal being jammed by at least 3 dB.

C. BROADCAST TV (VIDEO)

A decent TV picture has an SNR exceeding +20 dB. A TV picture with an SNR <3 dB reveals no discernible information, save for the occasional sync bars rolling through the image. Synch signals are peaks in the video signal and synch circuits are relatively narrowband, hence the synch is “the last to go.” TV images versus SNR are shown in Figure 25.

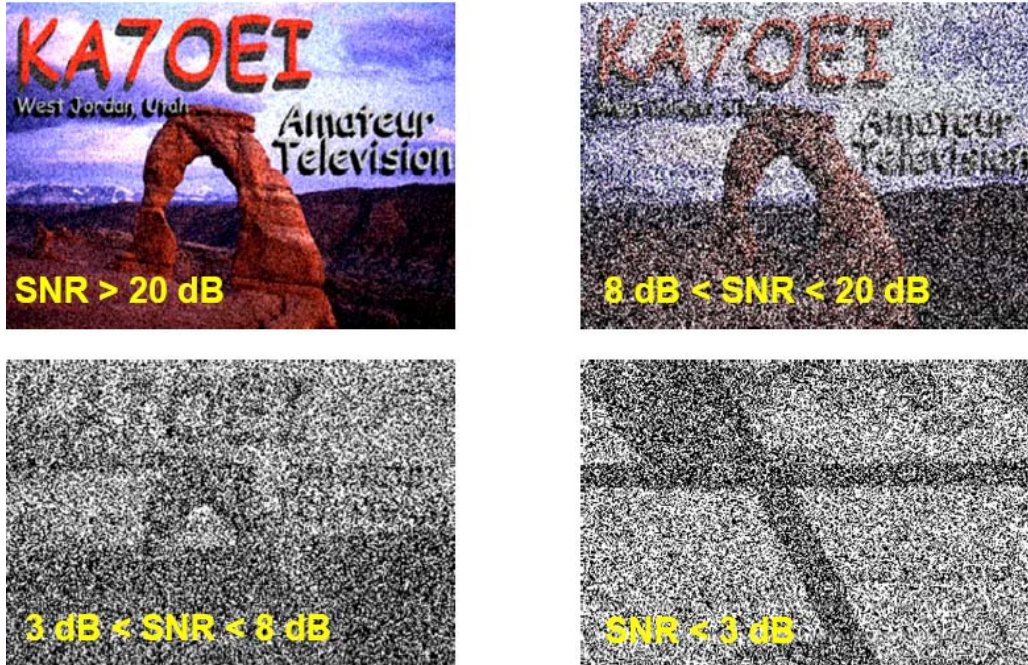


Figure 25. Image Quality versus SNR (After Ref. [18].)

D. BROADCAST TV (AUDIO)

TV uses narrowband FM for its sound. Narrowband FM is more resilient to noise than video. However, the FM threshold effect occurs for CNR between 8 and 10 dB and FM receiver performance deteriorates rapidly for values lower than the threshold. The SNR for VSB (or non-coherent detection) cannot exceed the CNR. Therefore, at CNRs lower than +3 dB, both TV picture and TV sound are rendered useless to the viewer.

In summary, communications and broadcasting systems are designed to work with substantial signal-to-noise ratios. For example, for FM radio and TV broadcasting, the CNR is typically more than 30 dB over the intended coverage region. Therefore, $1/\text{CNR}$ is typically a small number (1/1000) and can be approximated conservatively the CJNR as

$$\frac{1}{\text{CJNR}} \approx \frac{1}{\text{CJR}}.$$

The above approximation signifies total reliance on jamming, and not on the combination of jamming and noise, to render the targeted signal unusable.

The following tables summarized the Jamming Objectives for Targeted Signals:

Target Signal	Jamming Signal	Modulating Signal	Threshold
AM Radio	AM	Audio Noise	CJNR < -12 dB
FM Radio	FM	Audio Noise	CJR < -3 dB
TV	AM-VSB	Video Noise	CJNR < +3 dB

Table 1. Threshold

Target Signal	Jamming Signal	Modulating Signal	Jamming Margin
AM Radio	AM	Audio Noise	$M_{dB} > 12$ dB
FM Radio	FM	Audio Noise	$M_{dB} > 3$ dB
TV	AM-VSB	Video Noise	$M_{dB} > -3$ dB

Table 2. Jamming Margin

VI. DEVELOPMENT OF THE MODEL

A. SITE-SPECIFIC AND STATISTICAL PREDICTIONS

It is commonly accepted that the propagation of communications and broadcast signals has the following three components:

- Large-Scale Path Loss,
- Log-Normal Shadowing, and
- Small-Scale Fading.

While large-scale propagation can be quantified deterministically, shadowing and small-scale fading result in random variables with associated probability density functions. Therefore, because of shadowing and small-scale fading, calculation of powers at the receiver input requires a probabilistic approach.

Log-normal shadowing describes the variation of the signal power at a constant distance from the transmitter, but in different directions from the transmitter. This is caused by variations in building height, size and material, separation between buildings, presence of trees, etc. Therefore, the generally accepted model for shadowing is the non-zero mean normal (Gaussian) distribution for the signal amplitude/power expressed in decibels, hence, the name “log-normal shadowing.” The mean value of the (signal power) log-normal random variable is the power (in dB) calculated from the large-scale propagation model. The standard deviation for the log-normal shadowing is generally accepted to be 6 dB and 12 dB, depending on the environment type (i.e. rural, suburban, urban).

The small-scale fading model accounts for multipath propagation in the vicinity of the receiver. The commonly accepted model for multipath fading is the Rayleigh model.

For a dominant path with a substantially higher signal power than other paths, the Rice model is commonly applied. The Rice model may apply to TV reception because of the use of directional (moderate gain) antennas, such as Yagi-Uda parasitic arrays (Yagis) or Log-Periodic Arrays (LPAs) which are often aimed directly at the transmitter (line-of-

sight propagation). The Probability Density Function (PDF) for the signal amplitude for the Rayleigh model is the Rayleigh PDF. The PDF for the power of the Rayleigh-distributed signal amplitude is the Exponential PDF.

Considering the attributes of the three propagation models that were mentioned, only large-scale path loss lends itself to site-specific prediction techniques for typical jamming scenarios. Shadowing cannot be predicted using site-specific techniques because:

- exact locations of the receivers are not known in general,
- receiver surroundings are typically not known in sufficient detail, and
- even if the above information were available, the computational effort to calculate the power at a typically large number of targeted receiver locations would be prohibitive.

Whereas shadowing involves receiver surroundings on the scale of tens to thousands of wavelengths, small-scale fading depends on the details of the surroundings on the scale of several wavelengths. Therefore, the level of details for site-specific fading prediction would be even more demanding than for site-specific shadowing prediction.

Therefore, the bottom line is to rely on statistical techniques to account for shadowing and small-scale fading. While site-specific predictions for the “area mean values” are possible, they are dependent on the availability of reliable software, computational resources and digital maps of the target area. A number of well-regarded and validated models do exist for large-scale path loss prediction. Eventually, for jamming applications, the only realistic choice between site-specific and statistical predictions applies to large-scale path loss prediction. Shadowing and small-scale fading have to be, in practice, accounted for by statistical models.

B. LOG-NORMAL SHADOWING

Both theoretical and measurement based propagation models indicate that average received signal power decreases logarithmically with distance, whether in outdoor or indoor radio channels. Such a model is used extensively and is called Power Law or Log Distance Path Loss Model. This average loss for an arbitrary transmitter and receiver separation is expressed as a function of distance by using a path loss exponent as [19]

$$\overline{PL}(d) \propto \left(\frac{d}{d_o}\right)^n, \quad (6.1)$$

$$\overline{PL}(\text{dB}) = \overline{PL}(d_o) + \left(10 \times n \times \log\left(\frac{d}{d_o}\right)\right), \quad (6.2)$$

where

- n = path loss exponent,
- d = transmitter receiver separation distance, and
- d_o = close-in reference distance.

The path loss exponent indicates the rate at which the path loss increases with distance. The close-in reference distance is determined from measurements close to the transmitter. The bar denotes the ensemble average of all possible path loss values for a given distance.

The above mentioned equation, however, does not consider the fact that the surrounding environmental clutter may be vastly different at two different locations having the same transmitter and receiver separation. This leads to measured signals that are vastly different than the average value predicted by the power law. Measurements indicate that the path loss at a particular location is random and log-normally distributed about the mean distance dependent value, and is given as [19]

$$\overline{PL}(\text{dB}) = \overline{PL}(d_o) + \left(10n \log\left(\frac{d}{d_o}\right)\right) + X_\sigma \quad (6.3)$$

where X_σ = zero-mean Gaussian distribution random variable with standard deviation of σ .

The log-normal distribution describes the random shadowing effects, which occur over a large number of measurement locations that have the same transmitter and receiver separation, but have different levels of clutter on the propagation path. This phenomenon is referred to as Log-Normal Shadowing. In practice, the values of path loss exponent and standard deviation are computed from measured data, using linear regression such that the difference between the measured and estimated path losses is minimized in a

mean square error sense over a wide range of measurement locations and transmitter-receiver separations.

C. SMALL SCALE FADING

Small scale fading is used to describe the rapid fluctuations of the amplitudes, phases or multi-path delays of a radio signal over a short period of time or travel distance. The fading is caused by wave interference between various multi-path components that arrive at the receiver and combine vectorally to give the resultant signal, which can vary widely in amplitude and phase. Many physical factors in the radio propagation channel influence small-scale fading, such as [19, 20]

- transmission bandwidth of the signal,
- speed of the mobile unit,
- time delay spread of the received signal,
- random phase and amplitude, and
- mobile environment.

In a mobile radio channel, where either the transmitter or the receiver is immersed in cluttered surroundings, the envelope of the received signal typically has a Rayleigh distribution. The Rayleigh distribution has a probability density function given as [20]

$$p(r) = \frac{re^{-\left(\frac{r^2}{2\sigma^2}\right)}}{\sigma^2}, \quad \text{for } 0 \leq r \leq \infty \quad (6.4)$$

and

$$p(r) = 0, \quad \text{for } r < 0, \quad (6.5)$$

where σ^2 = variance of the received signal.

The Rayleigh probability density function for signal amplitude in terms of its average can also be expressed as

$$p(A) = \frac{\pi A}{2(\overline{A})^2} e^{-\left(\frac{\pi A^2}{4(\overline{A})^2}\right)}, \quad \text{for } 0 \leq A \leq \infty \quad (6.6)$$

and

$$p(A) = 0, \quad \text{for } A < 0, \quad (6.7)$$

where A = signal amplitude and over-bar denotes the average value.

The power of a Rayleigh distributed random variable has the exponential probability density function given as

$$p(P) = \frac{1}{\overline{P}} e^{-\left(\frac{P}{\overline{P}}\right)}, \quad \text{for } 0 \leq P \leq \infty \quad (6.8)$$

and

$$p(P) = 0, \quad \text{for } P < 0, \quad (6.9)$$

where P = power of the (signal) random variable and the over-bar denotes the average value.

When there is a dominant non-fading signal component present, the small scale fading distribution is Ricean, as in the case of line-of-sight propagation. In these cases, random components arriving at different angles are superimposed on a stationary signal giving the effect of adding an average value to the random multi-path. The Ricean distribution for such situation is given as [19]

$$p(r) = \frac{r}{\sigma^2} e^{-\frac{(r^2 + A^2)}{2\sigma^2}} I_0\left(\frac{Ar}{\sigma^2}\right), \quad \text{for } (A \geq 0, r \geq 0) \quad (6.10)$$

and

$$p(r) = 0, \quad \text{for } (r < 0), \quad (6.11)$$

where

- A = peak amplitude of the dominant signal, and
- I_0 = modified Bessel function of the first kind and zero order.

D. THE PROPOSED STATISTICAL MODEL

The jamming signal and the targeted signals are two independent random variables, that is, they are different signals with different sources and propagation paths. The ratio of the powers of two Rayleigh distributed random variables has the following probability density function:

$$p(R) = \frac{\bar{R}}{(R + \bar{R})^2}, \quad \text{for } 0 \leq R \leq \infty \quad (6.12)$$

and

$$p(R) = 0, \quad \text{for } R < 0, \quad (6.13)$$

where R = ratio of jamming and targeted signal powers at the Rx input and the over-bar indicates the average value.

The average value of the power ratio is also a random variable due to log-normal shadowing and can be represented in decibels as

$$\begin{aligned} R_{dB} &= 10 \log(\bar{R}) \\ &= 10 \log\left(\frac{P_j}{P_s}\right) \\ &= 10 \log(P_j) - 10 \log(P_s) \\ &= P_{jdB} - P_{sdB}, \end{aligned} \quad (6.14)$$

where P_{jdB} = jamming power in dB and P_{sdB} = targeted signal power in dB.

The power ratio, being the difference between two independent random variables, is a random variable with the mean and variance given by

$$\text{mean}(R_{dB}) = \overline{R_{dB}} = \overline{P_{jdB}} - \overline{P_{sdB}} \quad (6.15)$$

and

$$\text{variance}(R_{dB}) = \sigma_{Rdb}^2 = \sigma_{jdB}^2 + \sigma_{sdB}^2. \quad (6.16)$$

Also, the probability that the ratio of powers of two independent Rayleigh distributed random variables will exceed a non-zero positive threshold is given by

$$P(R \geq T) = \int_T^{\infty} p(R) dR \quad (6.17)$$

$$= \int_T^{\infty} \frac{\overline{R}}{(R + \overline{R})^2} dR$$

$$= \frac{\overline{R}}{T + \overline{R}}, \quad (6.18)$$

where T = threshold value.

All the values of the power ratio can also be integrated and after simplifying the integral through a series of transformations to get the following relationships:

$$P(R \geq T) = \frac{1}{2\pi} \int_{-\infty}^{+\infty} \frac{1}{1 + \alpha e^{-\beta x}} e^{-\frac{x^2}{2}} dx, \quad (6.19)$$

here

$$\alpha = \frac{10^{\frac{M_{dB}}{10}}}{10^{\left[\frac{(EIRP_{jdB} - EIRP_{TdB}) + (L_{TRdB} - L_{jRdB}) + (G_{RjdB} - G_{RTdB})}{10} \right]}}, \quad (6.20)$$

$$\beta = \ln \left(10^{\frac{\sqrt{\sigma_{jdB}^2 + \sigma_{sdB}^2}}{10}} \right), \quad (6.21)$$

and

$$T = 10^{\frac{M_{dB}}{10}}, \quad (6.22)$$

where

- $EIRP_{jdB}$ = jammer EIRP in dB,
- $EIRP_{TdB}$ = targeted transmitter EIRP in dB,
- L_{TRdB} = large scale path loss from the transmitter of the targeted signal to the targeted receiver in dB,
- L_{jRdB} = large scale path loss from the jammer to the targeted receiver in dB,
- G_{RTdB} = receiver antenna gain in the direction of the transmitter in dB,
- G_{RjdB} = receiver antenna gain in the direction of the jammer in dB, and
- M = required jamming margin in dB.

However, the integral in (6.19) can be evaluated by selecting a sufficient number of points ' x_n ' ($N_s > 100$) between the integration limits and calculating (if using uniformly distributed sampling points) the step Δx . The relationship becomes

$$P(\alpha, \beta) = \frac{1}{2} \sum_{n=0}^{N_s-1} \left[\frac{1}{1 + \alpha e^{-\beta x_n}} \left(\operatorname{erf} \left(\frac{x_n + \frac{\Delta x}{2}}{\sqrt{2}} \right) - \operatorname{erf} \left(\frac{x_n - \frac{\Delta x}{2}}{\sqrt{2}} \right) \right) \right] \quad (6.23)$$

and

$$P(\alpha, \beta) = \frac{\Delta x}{\sqrt{2\pi}} \sum_{n=0}^{N_s-1} \left[\frac{e^{-\frac{(x_n)^2}{2}}}{1 + \alpha e^{-\beta x_n}} \right]. \quad (6.24)$$

The above formulas can now be used in a given scenario. For example, given the parameters

- The transmitter EIRP is 10 dB higher than the jammer EIRP,

- Jammer-to-receiver path loss is 6 dB lower than the transmitter-to-receiver path loss,
- The receiver antenna gains towards the jammer and transmitter are equal,
- The standard deviation for the log-normal shadowing is 8 dB for both the jammer and transmitter signal,
- The required jammer margin is 3 dB, then
- The values of α and β for the above parameters are

$$\alpha = 5.012$$

$$\beta = 2.605.$$

Using these formulas, the probability of the jamming signal exceeding the target signal by the required margin is 0.304 or 30.4%. This probability of exceeding the jamming margin can also be interpreted as the percentage of the receivers that would be jammed within the target area. Therefore, in the given example, 30.4% of the receivers will be jammed.

However, the implicit assumption here is that the target area radius is small compared to the distances between the transmitter and the jammer, such that the powers calculated from the large-scale path models apply to all receivers within the target area.

THIS PAGE INTENTIONALLY LEFT BLANK

VII. CONCLUSIONS

A. CONCLUSIONS

The goal of this research was to develop a statistical model to calculate the effectiveness of an airborne jammer on communications and broadcast receivers.

Based on the example and from performing similar calculations for different combinations of relevant parameters using the model, it is concluded that it is quite difficult to achieve high probabilities of exceeding the typical required jamming margins. The main issue is that the EIRP of the transmitter could be substantially higher than the EIRP of the jammer, especially when jamming broadcast receivers. It may not always be possible to offset this disadvantage by moving the jammer closer to the targeted area. The problem could be further aggravated if the targeted receivers are using directional antennas pointed towards the transmitter, as may be the case for broadcast TV receivers with roof-top antennas.

B. RECOMMENDATIONS

The solution may be to use spatial diversity jamming, that is, to use two or more jammers spaced sufficiently far apart from each other such that their jamming signals at the targeted area are de-correlated due to the differences in their respective angles of arrival as shown in Figure 26.

The jamming signals should be of the same type; for example, if jamming an FM target signal, all jamming signals should be FM, at the same carrier frequency, but could be independent from each other.

The probability that two jamming signals be within the threshold at the same time will be the product of their respective probabilities, that is, it will be reduced, meaning that the probability of at least one signal exceeding the threshold will be increased.

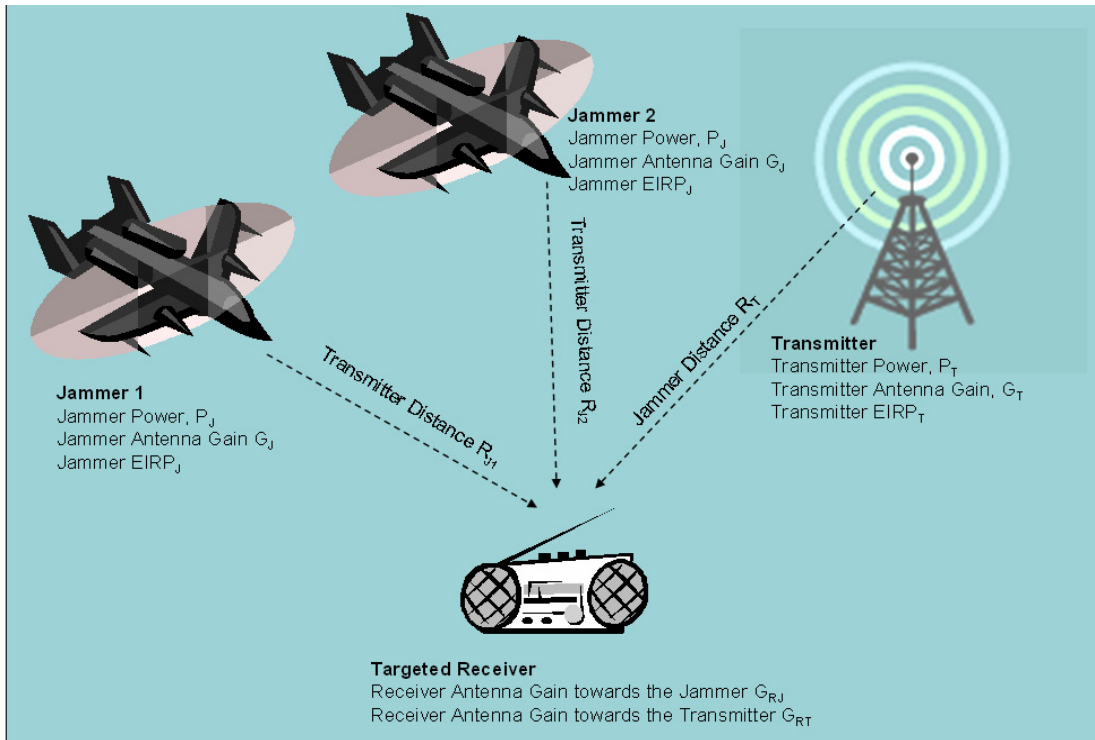


Figure 26. Spatial Diversity Jamming

LIST OF REFERENCES

- [1] A. MacLean, *Ideas on Jamming Digital Communications Analog*, <http://www.maclea-nj.com/opinions/stories/2.htm>, accessed 21 July 2005.
- [2] S. Tabbanne, *Handbook of Mobile Radio Networks*, Artech House Publishers, Norwood, MA, 2000.
- [3] R. Steele and L. Hanzo, *Mobile Radio Communications*, John Wiley & Sons Ltd., West Sussex, England, 1999.
- [4] *Wireless Communication*, Baltzer Science Publishers, Interactive Multimedia CD-ROM, Vol. 1, No.1, Amsterdam, ISSN 1383 4231, 1996, http://people.deas.harvard.edu/~jones/es151/prop_models/propagation.html, accessed 21 March 2005.
- [5] K. Siwiak, *Radio Propagation and Antennas for Personal Communications*, Artech House Publishers, Norwood, MA, 1998.
- [6] D. Adamy, *EW 102: A Second Course in Electronic Warfare*, Artech House Publishers, Norwood, MA, 2004.
- [7] B. Sklar, *Digital Communications*, Prentice Hall, Upper Saddle River, 2001.
- [8] M.L. Skolnik, *Introduction to Radar Systems*, McGraw Hill, Boston, MA, 2001.
- [9] S. Haykin, *Communication Systems*, John Wiley & Sons, Inc., New York, 1994.
- [10] P.Z. Peebles, Jr., *Communication System Principles*, Addison-Wesley Publishing Company, Inc., Massachusetts, 1976.
- [11] W.D. Gregg, *Analog and Digital Communication*, John Wiley & Sons, Inc., New York, 1977.
- [12] *Frequency Modulation*, Wikipedia, The Free Encyclopedia, http://en.wikipedia.org/wiki/Frequency_modulation, accessed 20 April 2005.
- [13] A.R. Hambley, *An Introduction to Communication Systems*, Computer Science Press, New York, 1989.
- [14] L.W. Couch, II, *Digital and Analog Communication Systems, 2nd Ed.*, Macmillan Publishing Company, New York, 1987.
- [15] S. Haykin, *Communication Systems*, John Wiley & Sons, Inc., New York, 1994.

- [16] K4Y TZ, *Electronics for Radio Amateurs*, York County Amateur Radio Society, <http://www.ycars.org>, accessed 20 April 2005.
- [17] Adapted from *Computer Aided Systems Human Engineering*, Crew System Ergonomic Information Analysis Center, Wright-Patterson Air Force Base, v. 1.0, <http://www.meyersound.com/support/papers/speech/mbn.htm>, accessed 10 June 2005.
- [18] *IF Bandpass Filtering of AM TV Signals*, Utah ATV Home Page, http://www.ussc.com/~uarc/utah_atv/if_filt.html, accessed June 2005.
- [19] T.S. Rappaport, *Wireless Communications – Principles and Practice*, Prentice Hall, Inc., New Jersey, 2002.
- [20] J.D. Gibson, *The Mobile Communications Handbook*, CRC Press, USA, 1996.

INITIAL DISTRIBUTION LIST

1. Defense Technical Information Center
Ft. Belvoir, Virginia
2. Dudley Knox Library
Naval Postgraduate School
Monterey, California
3. Professor Dan Boger, Chairman
Department of Information Sciences
Naval Postgraduate School
Monterey, California
4. Professor Jovan E. Lebaric
Department of Electrical and Computer Engineering
Naval Postgraduate School
Monterey, California
5. Professor Richard W. Adler
Department of Electrical and Computer Engineering
Naval Postgraduate School
Monterey, California
6. Narciso A. Vingson, Jr.
CDR, Philippine Navy
Headquarters Philippine Navy
Manila
7. Vaqar Muhammad
LCDR, Pakistan Navy
Pakistan